

OPTIMISING LOWER LAYERS OF THE PROTOCOL STACK TO  
IMPROVE COMMUNICATION PERFORMANCE IN A WIRELESS  
TEMPERATURE SENSOR NETWORK

by

RACHEL KUFAKUNESU

submitted in accordance with the requirements for the degree of  
MAGISTER TECHNOLOGIAE: ENGINEERING: ELECTRICAL

DEPARTMENT OF ELECTRICAL & MINING ENGINEERING  
UNIVERSITY OF SOUTH AFRICA

Supervisor: Prof. M.O. Ohanga

30<sup>th</sup> October 2018

DECLARATION

Name: Rachel Kufakunesu

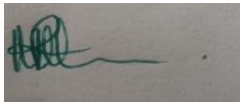
Student Number: 47062096

Degree: Master of Technology

Exact wording of the title of the dissertation as appearing on the copies submitted for examination:

Optimising Lower Layers of the Protocol Stack to Improve Communication Performance in a Wireless Temperature Sensor Network

I declare that the above dissertation is my own work and that all the sources that I have used or quoted have been indicated and acknowledged by means of complete references.



30<sup>th</sup> October 2018

.....

.....

Signature

Date

## ABSTRACT

The function of wireless sensor networks is to monitor events or gather information and report the information to a sink node, a central location or a base station. It is a requirement that the information is transmitted through the network efficiently. Wireless communication is the main activity that consumes energy in wireless sensor networks through idle listening, overhearing, interference and collision. It becomes essential to limit energy usage while maintaining communication between the sensor nodes and the sink node as the nodes die after the battery has been exhausted. Thus, conserving energy in a wireless sensor network is of utmost importance.

Numerous methods to decrease energy expenditure and extend the lifetime of the network have been proposed. Researchers have devised methods to efficiently utilise the limited energy available for wireless sensor networks by optimising the design parameters and protocols. Cross-layer optimisation is an approach that has been employed to improve wireless communication. The essence of cross-layer scheme is to optimise the exchange and control of data between two or more layers to improve efficiency. The number of transmissions is therefore a vital element in evaluating overall energy usage.

In this dissertation, a Markov Chain model was employed to analyse the tuning of two layers of the protocol stack, namely the Physical Layer (PHY) and Media Access Control layer (MAC), to find possible energy gains. The study was conducted utilising the IEEE 802.11 channel, SensorMAC (SMAC) and Slotted-Aloha (S-Aloha) medium access protocols in a star topology Wireless Temperature Sensor Network (WTSN). The research explored the prospective energy gains that could be realised through optimizing the Forward Error Correction (FEC) rate. Different Reed Solomon codes were analysed to explore the effect of protocol tuning on energy efficiency, namely transmission power, modulation method, and channel access. The case where no FEC code was used and analysed as the control condition.

A MATLAB simulation model was used to identify the statistics of collisions, overall packets transmitted, as well as the total number of slots used during the transmission phase. The bit error probability results computed analytically were utilised in the simulation model to measure the probability of successful transmitting data in the physical layer. The analytical values and the simulation results were compared to corroborate the correctness of the models. The results indicate that energy gains can be accomplished by the suggested layer tuning approach.

## ACKNOWLEDGEMENTS

I wish to convey my heartfelt appreciation to my supervisor Prof. Marcel Odhiambo Ohanga for his guidance and valuable advice throughout the course of my studies. Additional thanks go to Dr. Tebello Mathaba for his assistance and advice on MATLAB programming. Financial support from the UNISA Student Funding Department (DSF-POSTGRD) is gratefully acknowledged.

I wish to acknowledge my family and friends for their moral support and encouragement during my studies. A special thank you goes to my husband, Rodwell Kufakunesu for his support, understanding and encouragement, for his patience in explaining difficult Mathematical concepts. Without your love and support I would not have completed this dissertation. To my children Gwyneth, Nigel and Valerie, thank you for giving me time to study, foregoing homework supervision and playtime. I love you.

Lastly, but certainly not least, I would like to give thanks to God Almighty, for sustaining me throughout the duration of my studies, with whom all things are possible.

## TABLE OF CONTENTS

DECLARATION	i
ABSTRACT	ii
ACKNOWLEDGEMENTS	iii
LIST OF FIGURES	viii
LIST OF TABLES	ix
TERMINOLOGIES	x
NOTATIONS	xii
CHAPTER ONE: INTRODUCTION	1
1.1 Overview of the Research	1
1.2 Purpose of the Study	5
1.3 Research Objectives	5
1.4 Scope of the Research	5
1.5 Thesis Organisation	5
CHAPTER TWO: LITERATURE REVIEW	6
2.1 Introduction	6
2.2 Problem Statement	6
2.3 Review of Layer Optimisation Schemes	6
2.3.1 Physical Layer Optimisation	7
2.3.2 MAC Layer Optimisation	8
(i) SensorMAC (SMAC) Protocol	9
(ii) Timeout-MAC (TMAC) Protocol	10
(iii) Sift Protocol	10
(iv) WiseMAC Protocol	11
(v) Traffic Adaptive MAC Protocol	11
(vi) Berkeley-MAC (B-MAC) Protocol	12
2.3.3 Cross-Layer Optimisation	12
(i) Energy Constrained Path Selection (ECPS) Protocol	12
(ii) Cross-Layer MAC (MAC-CROSS) Protocol	13
(iii) Transmission Scheme Optimisation Protocol	13
(iv) Joint Routing MAC and Link Layer Optimisation Protocol	14
(v) Unified Cross-Layer (XLP) Protocol	14

(vi) Energy Optimisation Approach (EOA) Protocol	15
(vii) PHY and MAC Layer Optimisation Protocol	15
(viii) ERI-MAC Protocol	16
(ix) Energy Harvesting (EH) Protocol	16
2.4 Proposed Solution	18
2.5 Chapter Conclusion	18
CHAPTER THREE: ANALYSIS OF THE PROPOSED SOLUTION	19
3.1 Introduction	19
3.2 Proposed Solution	19
3.3 Components of the Proposed Solution	20
3.4 Function of the Components of the Communication System	20
3.5 Optimising Physical and MAC Layers	22
3.6 Wireless Sensor Network	23
3.7 The 802.11g Channel	24
3.8 Physical Layer	25
3.8.1 Error Control Coding	26
3.8.2 Reed Solomon Codes	29
3.9 MAC Layer	30
3.9.1 SensorMAC Protocol	30
3.9.2 Slotted Aloha Protocol	31
3.10 Network Traffic	32
3.11 Markov Chains	32
3.12 Chapter Conclusion	34
CHAPTER FOUR: DESIGN OF THE PROPOSED SOLUTION	35
4.1 Introduction	35
4.2 Research Design	35
4.3 Network Setup	36
4.4 Transmission Period	37
4.5 Physical Layer Tuning	38
4.6 MAC Layer Tuning	40
4.7 Network Traffic Generation	41
4.8 Markov Chain Model	41

4.9	Time to Absorption	43
4.10	Transmission Period Analysis	44
4.11	Energy Consumption	45
4.12	Design Specifications for Implementation	47
4.13	Chapter Conclusion	47
CHAPTER FIVE: IMPLEMENTATION		49
5.1	Introduction	49
5.2	Simulation Environment	50
5.3	Simulation Details	52
5.4	Chapter Conclusion	53
CHAPTER SIX: SIMULATION TESTS AND RESULTS		54
6.1	Introduction	54
6.2	Simulation Tests	54
6.2.1	Bit Error Probability	55
6.2.2	Packet Success Probability	56
6.2.3	Number of Steps to Absorption	57
6.2.4	Number of Transmissions to Absorption	58
6.2.5	Time to Absorption	59
6.2.6	Energy Saving	61
6.2.7	Comparison of MAC Methods	62
6.3	Chapter Conclusion	62
CHAPTER SEVEN: ANALYSIS OF TEST RESULTS		63
7.1	Introduction	63
7.2	Bit Error Probability	63
7.3	Packet Success Probability	63
7.4	Number of Steps to Absorption	65
7.5	Number of Transmissions to Absorption	66
7.6	Transmission Time Saving	66
7.7	Energy Saving	67
7.8	Comparison of MAC Methods	68
7.9	Chapter Conclusion	68

CHAPTER EIGHT: CONCLUSION	68
8.1 Introduction	68
8.2 Applications for the Research	68
8.3 Implications of the Research	68
8.4 Recommendations for Further Work	69
8.5 Chapter Conclusion	69
REFERENCES	70
APPENDICES	75
Appendix A BEP.m	75
Appendix B PHY Layer.m	76
Appendix C Markov Model.m	77

## LIST OF FIGURES

Figure 1:	Communication block diagram	20
Figure 2:	Wireless sensor node architecture	21
Figure 3:	Optimisation block diagram	23
Figure 4:	Star topology network	24
Figure 5:	Unlicensed frequency bands	24
Figure 6:	Structure of the physical layer	26
Figure 7:	802.11 packet format	26
Figure 8:	Forward error correction scheme	28
Figure 9:	Reed Solomon code	29
Figure 10:	SMAC sleep-active cycle	31
Figure 11:	Slotted-Aloha protocol	32
Figure 12:	Probability transition diagram for a 3-state Markov chain	34
Figure 13:	Simulation Environment Setup	51
Figure 14:	General Representation of WTSN Simulation	52
Figure 15:	Bit Error Probability versus Signal to Noise Ratio in dB	55
Figure 16:	Packet success probabilities vs $\frac{E_b}{N_o}$ in dB for uncoded and coded cases	56
Figure 17:	Average number of steps vs $\frac{E_b}{N_o}$ in dB calculated using theoretical and simulation models with different p values	57
Figure 18:	Average number of transmissions required to reach absorption state, simulation and analytical results	58
Figure 19:	Saving percentage in average number of steps versus $\frac{E_b}{N_o}$ in dB for different code rates, p=0.05	59
Figure 20:	Average time saving percentage versus $\frac{E_b}{N_o}$ in dB for different code rates, p=0.05	60
Figure 21:	Energy saving percentage result versus $\frac{E_b}{N_o}$ in dB when using different code rates, p=0.05	61
Figure 22:	Comparison of energy consumption between S-Aloha and SMAC Medium Access protocols	62

## LIST OF TABLES

Table 1:	Physical Layer Characteristics for the Transceivers	38
Table 2:	Values for Generating Network Traffic	41
Table 3:	Parameter Values Used for Performance Evaluation	47
Table 4:	Simulation Tests and Results Obtained	54
Table 5:	BEP Performance for Uncoded and Coded PHY Protocol	55
Table 6:	Comparison of Packet Success Probability	56
Table 7:	Number of Steps to Absorption	57
Table 8:	Number of Transmissions to Absorption	58
Table 9:	Percentage Saving on Average Number of Steps	59
Table 10:	Transmission Time Saving Percentage	60
Table 11:	Energy Saving Percentage	61
Table 12:	Comparison of MAC Methods Energy Consumption in Joules	62

## TERMINOLOGIES

Bit Error Rate:	The percentage of bits that have errors relative to the total number of bits received in a transmission, an indication of how often a packet or other data unit must be retransmitted because of an error.
BCH Code:	Bose–Chaudhuri–Hocquenghem codes are a class of cyclic random error-correcting codes.
BPSK Modulation:	Binary Phase Shift Keying is a digital modulation technique used for data encoding in the phase of a reference signal.
Cross Layer Optimization:	One of the optimization techniques, in which different factors from different layers are considered to optimize the performance of the network.
CSMA/CA:	Carrier Sense Multiple Access with Collision Avoidance (CSMA/CA) defers a transmission of data by a random interval, contention window, thereby reducing the congestion on a channel.
Energy Efficient Protocols:	Protocols whose main objective is to minimise energy consumption.
ECC:	Error Control Coding - an assortment of digital signal processing methods used to regulate the effects of channel noise over several transmitted signals.
FEC:	Forward Error Correction is a technique of finding and controlling errors in the transmission of data where redundant data sent from the transmitter to the receiver identifies only the section of the data that does not contain evident errors.
Galois Field:	Galois field is another name for finite field. It is a field in which the number of elements is of the form $p^n$ , where $p$ is a prime number and $n$ is a positive integer, is called a Galois field, such a field is denoted by $GF(p^n)$ .
MAC Protocols:	Protocols that manage the transmissions and receptions of the radio on a shared medium of transmission providing connections for the overlying routing protocol.

Markov Chain:	It is a type of stochastic process which describes the order of possible events in which the probability of each event hinges only on the state reached in the preceding event.
MATLAB:	It is a high-performance software, MATrix LABoratory used for technical computing. It is an integration of numerical computation, visualisation and programming in an easy environment where mathematical notation is used to find solutions to problems.
OFDM Modulation:	Orthogonal Frequency Division Multiplexing scheme is a digital modulation scheme that uses multiple subcarriers within the same single channel to transmit data in parallel, rather than transmitting with a single subcarrier.
PHY Protocols:	Protocols defined for the medium of transmission of information from a source to a receiver.
S-Aloha	Slotted -Aloha is a medium access control protocol that does not perform carrier sensing during data transmission but synchronises the transmission within time-slots.
SMAC:	Sensor Media Access Control employs a duty cycle that is synchronised and a planned intermittent wake and sleep cycle
Stochastic Process:	It is a collection of random variables indexed by time. A random process that evolves with time, which can be discrete or continuous.
Symbol:	The current state of some observable signal which persists for a fixed period of time, having a specific phase, magnitude and frequency.
TDMA:	Time Division Multiple Access, one of the MAC protocols which the time is multiplexed among several nodes.
Throughput Efficiency:	the ratio between the effective delivered bit rate of a sink node to the offered or attempted bit rate at a source node. Throughput may be referred as good put in some analysis.
Wireless Sensor Network:	A set of wireless sensors which are deployed in a specific region. The sensor nodes cooperate with each other to forward data to the final destination.

## NOTATIONS

Description	Symbol
Average number of steps to adoption when the initial state $S=0$	$\Gamma_0$
Number of nodes with a new packet arrival	$K$
Fundamental matrix for absorbing chain	$\Lambda$
State transition probability matrix	$\mathbf{P}$
Events per second in a Poisson process	$\rho$
Time period for Poisson process	$\tau$
Average packet arrival rate	$\Theta$
Time to absorption for code rate $i$	$\Theta_i$
Energy per uncoded bit	$\varepsilon_{b,o}$
Energy per uncoded bit for code rate $i$	$\varepsilon_{b,i}$
Energy per symbol	$\varepsilon_s$
Number of arrivals according to a Poisson distribution	$\zeta$
Number of bits in RS coded symbol	$B$
Length of the data packet	$D$
Length of data packet when using code rate $i$	$D_i$
MAC layer imperfections effect in the energy consumption	$E_{Imp}^{MAC}$
MAC layer factor in the energy consumption of the receiver (sink)	$E_{rx}^{MAC}$
MAC layer factor in energy consumption of the Tx-node, failed transmission	$E_{tx,f}^{MAC}$
MAC layer factor in energy consumption of Tx-node, successful transmission	$E_{rx}^{MAC}$
PHY layer factor in the energy consumption of the receiver (sink)	$E_{tx}^{PHY}$
PHY layer factor in the energy consumption of the Tx-node	$E_{rx}^{PHY}$
Energy per bit to noise ratio	$E_b/N_o$
Network energy consumption during a transmission period for code rate $i$	$E_{TP,i}$
Network energy consumption during a transmission period	$E_{TP}$

Offered traffic load	$G$
Offered traffic load at state $j$	$G_j$
Markov chain model state $j$	$J$
Number of information symbols in a code word	$K$
Number of nodes with a packet to transmit	$M$
Average number of steps at state $j$ (without new arrivals)	$N_{steps,j}$
Average number of transmissions (without new arrivals) at state $j$	$N_{tx,j}$
Average number of transmissions (without new arrivals) to reach the absorption state	$N_{tx,MC}$
Number of successful transmissions	$n_{tx}^{succ}$
Number of failed transmissions	$n_{tx}^{fail}$
Probability to transmit in a slot	$P$
Probability of unsuccessful channel access (MAC layer)	$P_{fail}^{MAC}$
Probability of successful channel access (MAC layer)	$P_{succ}^{MAC}$
Unsuccessful transmission probability (PHY layer)	$P_{fail}^{PHY}$
Successful transmission probability (PHY layer)	$P_{succ}^{PHY}$
Probability of event $x$ during the transmission period	$P(x)$
Probability that $\Omega$ nodes have a new packet to transmit	$(P_{\Omega}(\Omega = \kappa))$
Error correction capability in symbols	$T$
Data frame duration for code rate $i$	$T_{f,i}$
ACK packet duration	$T_{ACK}$
Length of the idle slot	$T_{idle}$
Maximum waiting time for ACK packet	$T_{MaxAckWait}$
Slot length when using code rate $i$	$T_{slot,i}$
Symbol duration	$T_{sym}$
Number of code symbols in a packet when using code rate $i$	$X_i$
Number of nodes that will try to transmit in a slot	$X$

## CHAPTER ONE: INTRODUCTION

### 1.1 Overview of the Research

A wireless sensor network (WSN) is a wireless set of nodes expansively distributed, that uses sensors to record physical quantities such as temperature, pressure, motion and sound in the environment. The sensor nodes connect with routers that link to a gateway to create a quintessential wireless sensor network. The sensor nodes wirelessly communicate to a default gateway, which affords a link to the wired network where one could gather, develop, scrutinise, and present the data that has been measured.

A wireless sensor network is made up of many tiny, lightweight and transferable recognition bases called sensor nodes [1]. Each sensor node consists of a power source, transducer, transceiver and microcomputer. The transducer produces electrical pulses depending on the phenomena it is sensing. The microcomputer handles the sensor output and stores it. The transceiver is responsible for receiving instructions from the main computer as well as transmitting data from the sensors to the computer. The battery provides the power for each sensor node [1]. Since WSNs are application specific, their design and deployment take into account the intended purpose. Sensor networks are principally data-centric rather than location driven. Generally, numerous sensor nodes in their thousands are installed in the environment being monitored. Building a global addressing scheme would not be possible and as such the conventional IP-based routing protocols are not applicable. Queries are channelled to an area comprising a cluster of sensor nodes as opposed to particular sensor addresses. Because the sensors are in close proximity, the data they obtain could be similar, resulting in data aggregation being locally performed. This means, an aggregator node prepares an analysis and summarises the local data in the cluster, thereby decreasing the communication bandwidth requisites. Accuracy levels are increased, and the incorporation of data redundancy compensates for the node failures. Sensor node clusters and hierarchical networking allows the efficient utilisation of resources, reduction in consumption of power, ensures robustness and scalability, which are some of the crucial issues in wireless sensor networks [2]. WSN protocols utilise five layers in the Open Systems Interconnection (OSI) model, namely:

- (i) Application Layer.
- (ii) Transport Layer.
- (iii) Routing Protocol on the Network Layer.
- (iv) MAC Protocol on the Data Link Layer.

(v) Physical Layer

Each of the layers are assigned a task to execute autonomous of the other protocol stack layers. The layers in the protocol stack are arranged in a manner that maintains the restricted interface between adjacent layers, as such the arrangement can either be bottom-up or top-down. The architecture that is layered prohibits direct communication between layers that are not adjacent. The physical layer is the first layer of the protocol stack. It specifies and manages communication between different devices and their channel of communication. Frequency selection, carrier frequency generation, signal detection as well as modulation and data encryption, are the responsibilities of the physical layer. The data link layer as the next layer of the protocol stack, provides services that permit multiple nodes to successfully access and share a communication medium. These services comprise of medium access control, reliable delivery, error detection and error correction [3].

The third layer of the protocol stack, the network layer, establishes the communication pathways between nodes in a network and successfully routes the data packets along these pathways. The specifications of routing protocols may differ depending on the requirements of the network and hence a specific routing pathway would be preferable. For instance, some routing protocols enable the WSN to provide the best Quality of Service (QoS), others may select a pathway that will aid the wireless sensor network to secure the best lifetime, while others would favour a hybrid of both objectives. The transport layer is the fourth layer of the protocol stack, responsible for the reliable communication between application processes operating in the network devices. The application layer is the fifth and final layer, which is the layer that interfaces directly with the end-user of the network. Numerous protocols provide a service in the application layer including web surfing, web chat, simple mail transfer, file transfer, network management, email clients and virtual terminals. With regards to wireless sensor networks, the application layer processes the data that has been sensed, deals with encryption, data configuration and storage. Furthermore, the application layer scans through the underlying layers to ensure availability of network services and resources required to meet the end-user's specifications [4-7]. The session layer and the presentation layer of the OSI model are not utilised in wireless sensor networks. The authors in [8,9] provide a comprehensive insight on protocol layers of WSNs.

A WSN system is ideal for monitoring the environment where deployment is long term and often in difficult to reach places, for example, acquiring water, soil, or climate measurements. Wireless sensors can also be utilised on electricity grids, street lights, collecting health data, thereby reducing energy usage. The system can be used to effectively monitor structural health e.g. bridges, tunnels and highways. Office blocks, medical centres, airports, factories, industrial plants, or production facilities can also be monitored by WSN systems. Depending upon the application, the sensor nodes may incorporate additional supporting technologies, for example, a location discovering architecture to accurately establish their position, a mobiliser to alter the configuration or change the location of the sensor nodes etc.

A critical feature in the application of wireless sensor networks is the lifetime of the network. The network lifetime must be sufficient for the objective of the WSN to be achieved. The supply of power to the sensor nodes is limited, thus posing a big challenge in WSN deployment. Since wireless sensors depend on battery power for their operation, it is difficult to replace the batteries once the sensors are deployed in the field. This energy scarcity impacts on the network's localisation and routing protocols. The major activity that consumes energy in a WSN is wireless communication, that is, message size, transmission of messages, receiving messages, node awake time, and distance between nodes. The power utilisation of wireless devices greatly depends on the operations in the physical layer. The MAC layer, on the other hand, manages the wireless resources for the physical layer and therefore directly influences energy consumption. The MAC protocols contribute to energy depletion when there are collisions, overhearing, idle listening and through the control packets [10]. Numerous methods to curtail energy usage and therefore protract the lifetime of the network have been proposed.

Researchers have devised methods to efficiently utilise the limited energy available for WSN by optimising the design parameters and protocols. Significant work has been presented in the endeavour to minimise energy consumption at the MAC layer and it has been found that energy can be conserved in the physical layer by optimising its parameters such as the number of transmit antennas or the modulation scheme [11]. Although working with individual protocol stack layers helps in decreasing energy consumption in wireless sensor networks, it has been established that cross-layer optimisation of the complete stack results in the highest energy conservation. Cross-layer optimisation is the removal of the strict boundaries of the OSI layer and designing the layers in such a way that the dependence between the layers is exploited to

achieve an improvement in performance. This contrasts with the traditional layering where individual layers of the protocol stack are designed independently [12].

There are several perspectives in cross-layer design that have been put forward [13, 14, 15,16]. Disrupting the layered architecture of the OSI model is a way of designing the protocols using the cross-layer approach. This can be done, for instance, by permitting layers that are not adjacent to each other to communicate directly, or to share variables between them. This type of cross-layer approach that violates the layered structure is referred to as a design about the reference architecture. Several research papers consider the cross-layer interface, where the conventional layered configuration is maintained, whilst every layer is notified about the settings of the other layers. Nevertheless, the structure of each layer remains intact. Additionally, the protocol layers are amalgamated in order to present a single interface element for effective communication in wireless sensor networks. The most common cross-layer design developed is between the physical layer and the MAC layer compared to any combination of the other layers in the protocol stack. This is mainly because they are adjacent to each other. The techniques that have been employed in cross-layer design include the following categories among others:

- (i) Multiple coding and modulation schemes: The rate of transmission of a link is affected when the coding or modulation schemes are varied. [17,18].
- (ii) Advanced antenna techniques: The type of antennas used have bearing on the cross-layer design, for example directional antennas and smart antennas.
- (iii) Multiple Input Multiple Output (MIMO): MIMO can significantly increase the transmission rate of a wireless link using advanced signal processing techniques and multiple antennas for signal transmission and reception.

The focus of this research was on tuning the adjacent layers of the protocol stack, the physical layer and the MAC layer, to improve the communication performance in a WTSN using the Markov chain model and Reed Solomon forward error correction coding on an 802.11g channel with Additive White Gaussian Noise (AWGN). IEEE 802.11 is commonly known as Wi-Fi whose typical structure is the star topology, with many wireless stations connecting to an access Point (AP) that then connects to a network infrastructure. The MAC and PHY specifications for implementation are given in [19]. The key benefit of developing 802.11 sensing systems is its compatibility with already existing networks and infrastructure.

## 1.2 Purpose of the Study

The purpose of this study was to investigate an energy consumption model by jointly tuning the PHY and MAC layers of a WTSN, design and implement a mechanism that will provide, or results in energy savings in WTSNs. Thus, the proposed solution was to design and implement a mechanism that will conserve energy in WTSNs.

## 1.3 Research Objectives

- (i) The main objective of this research was to analyse existing energy saving solutions and propose a communication cross-layer mechanism approach that maximises energy efficiency in communication performance.
- (ii) The research evaluated and compared possible energy savings that could be accomplished by jointly enhancing the PHY and MAC layers.
- (iii) The research activity consisted of the design, implementation and testing of a mechanism that jointly enhances the PHY and MAC layers to achieve the first objective.

## 1.4 Scope of the Research

As described in the research overview section of this document, there are quite a few protocols designed in cross layers of the network protocol stack [13, 14, 15, 16]. However, the scope of this research was limited to cross layer design involving PHY and MAC layers to conserve energy in a single hop star topology wireless temperature sensor network.

## 1.5 Thesis Organisation

The thesis is organised into seven chapters. Chapter 1 provides the background information and introduction. The literature review and materials relevant to the study are covered in Chapter 2. Chapter 3 introduces the analysis of the proposed solution, that is, the notion of cross-layer design and proposed model. It breaks down the solution into sub-solutions and explains the function of each sub-solution. A description of the design of the solution is covered under Chapter 4, the processes and techniques of how to implement the proposed solution. Chapter 5 provides the implementation of the proposed solution, the techniques and procedures implemented, and the results obtained. A detailed analysis of the test results is given in Chapter 6 and Chapter 7 concludes with an overview of the research and recommendations for future studies. The last section presents the reference sources used in this research.

## CHAPTER TWO: LITERATURE REVIEW

### 2.1 Introduction

Individual layer optimisation in wireless sensor networks has been the norm in the recent past until the advent of cross-layer optimisation. Enhancing individual protocol stack layers aids in reducing energy consumption in wireless sensor networks, it has been established that cross-layer optimisation of the entire stack will result in major improvement in energy conservation [12]. Cross-layer optimisation is the removal of the strict boundaries of the OSI layer and designing the layers in such a way that the dependence between the layers is exploited to achieve an improvement in performance. In this chapter, a review of the optimisation schemes is conducted, and a discussion of the benefits and shortcomings is presented.

Before reviewing optimisation schemes, the research problem and purpose, research objectives and scope of the research are presented.

### 2.2 Problem Statement

In wireless sensor networks conserving energy is of greatest significance because sensor nodes will die after the battery has been exhausted [1]. The major activity that consumes energy in a WTSN is wireless communication [2]. Energy is expended by the message size, transmission of messages, receiving messages, node awake time and distance between nodes [17]. The power consumption of wireless devices greatly depends on the physical layer. The MAC layer manages the wireless resources for the physical layer and directly influences the energy consumption. The MAC protocols contribute to energy depletion when there is idle listening, overhearing, collisions and through the control packet overhead. Optimising the responsible layers on the protocol stack will address the challenge of network lifetime. Communication protocols need to be as energy efficient as possible to do this. Energy is a scarce resource in WTSNs and hence the need to preserve energy in order to extend the network lifetime.

### 2.3 Review of Optimisation Schemes

Conventionally, optimisation of energy expenditure has been considered at individual layers of the protocol stack. Cross-layering, however, has provided the capability of simultaneously using data from various layers of the protocol stack, hence improving efficiency.

### 2.3.1 Physical Layer Optimisation

Operation of the radio circuitry and transmitting the data bit stream consumes the bulk of the energy in wireless sensor networks. The energy utilised by the operation of the radio circuitry is fixed, while that used for data transmission varies depending on transmission distance, interference and channel loss [20]. The physical layer design technologies are dependent on bandwidth, radio architecture and modulation schemes. The start-up time of the physical layer was considered in [21], which demonstrated the importance of evaluating the physical layer's start-up time as it has a correlation with energy efficiency of the system. The energy used at start-up influences the energy expended in a transmission. The researchers experimented with different modulation schemes and showed that certain start-up times had preferable modulation schemes that significantly saved energy.

Transmission power and circuit power consumption were considered in [22]. The authors offered comprehensive study around the consumption of power by the mechanisms of the transmitter and receiver devices. Their conclusion was that, given short transmission distances, schemes that are bandwidth-efficient are energy efficient. Bandwidth-efficient schemes have linear modulations with large constellation sizes that are uncoded. In contrast, coded nonlinear modulation with large constellation sizes, which are energy-efficient schemes, are energy efficient at large transmission distances. Their assumption was to pursue a static bit error probability and no retransmission. This assumption though, might not satisfy some QoS needs like reliable communication. Authors in [23] provided analytical models for establishing the range of transmission that utilises the least energy in homogenous node distribution. They used a universal transmission range for all the nodes to determine the mean per hop packet progress and then use this result to ascertain the optimum per hop transmission range that delivers maximum energy efficiency using their analytical model. They discovered that large radio transmission range enhances the expected progress of data packets towards its destination at the expense of higher energy consumption per short transmission range, but on the contrary consumes less per transmission energy even though it results in a larger number of hops for a data packet to reach its destination. Their work however, did not consider multiple traffic flows caused by retransmissions. Multiple traffic flows mean additional energy utilisation as a result of the retransmissions which may ultimately affect the transmission range optimisation. They also assumed a uniform transmission radius which is not always practical.

In [24], the authors analysed the challenge of energy-efficient transmission of data over a noisy channel concentrating on adjusting the parameters in the physical layer. The authors derived a metric that stipulated the projected energy required to successfully transmit a bit over a specific distance given a channel noise model and called it the Energy Per Successfully Received Bit (ESB). Through decreasing the metric ESB, the authors calculated the energy-optimum relay distance as well as the optimal transmission energy as a function of the path loss exponent and channel noise level using different modulation schemes. The results obtained allow network designers to maximise the network lifetime by manipulating the hop distance, modulation scheme and/or the transmit power. The authors studied the impact of fluctuating the Bit Error Rate (BER) to obtain the parameters of the physical layer that minimise the amount of energy required to receive the data successfully. The authors considered a Rayleigh fading channel model and the Additive White Gaussian (AWG) channel model.

The simulation results showed that the optimal hop distance for the node to get sensed data to its destination could be calculated, along with the optimal transmission energy once the modulation scheme and the channel have been identified. Their study concluded that the employment of relay distance and optimal transmission energy is critical in accomplishing a wireless sensor network that is energy efficient. The authors determined that to achieve the best possible ESB, it would not be sufficient to optimise the transmission energy only without optimising the relay distance. Once the scheme was operational at the optimal distance, the other two metrics ESB and the transmission energy became impartial to channel noise. In this case, however, hop distance was fixed, but in actual networks, this distance is usually random. Considering real life wireless sensor networks, it would be impossible to locate all the nodes in a manner that guarantees that the nodes could employ the optimum hop distance, neither would it be possible to fix transmit power to the precise optimal point. In either case, the physical limitations of the architecture regarding the topology of the sensor field and the constraints of the hardware's precision would hinder the system from attaining this abstract optimal behaviour. The model could be improved by finding the optimum energy for a randomly distributed hop distance.

### 2.3.2 MAC Layer Optimisation

MAC protocols contribute to energy depletion when there is idle listening, overhearing, collisions and through the control packet overhead. MAC protocols need to be energy efficient, reliable, high throughput and low access latency, to prevent redundant power consumption.

One of the essential tasks of MAC protocols is to circumvent collisions to prevent nodes that are interfering from transmitting simultaneously. Optimising packet size in WSNs is another technique that was studied expansively. An algorithm was developed that allows Automatic Repeat Request Protocol (ARQ) to optimise the size of the data packets dynamically [25] dependent on the estimated channel BER. The authors developed a Markov chain model to investigate the performance of the system under constant channel conditions. The results showed that, using a history of just ten thousand bits, the system performance that is near optimum could be achieved. Link adaptation techniques were used to improve energy efficiency using variable frame size in [26]. The authors optimised the size of the data frame with reference to the quality of the channel. The proposed algorithm reduced retransmissions caused by frame errors and collisions. The dynamic frame size minimised energy usage and guaranteed quicker delivery. The authors made use of the Kalman filter to forecast the optimum packet size that improved goodput and energy efficiency, whilst minimising the requirement for sensor memory. The authors focused on the MAC layer, since it is the layer that is responsible for provision of access to the shared medium and data transmission over the physical channel. Their proposed algorithm resulted in up to fifteen percent improvement on energy efficiency without jeopardising the performance of the network. An analysis of energy saved from dynamic packet length with various modulations regarding range, goodput, and energy consumption were carried out in [27].

The use of fixed size packets was suggested in [28] wherein the authors established the optimum fixed packet size by maximising the energy efficiency metric, for a particular array of channel and radio parameters. The authors examined the consequence of using error control on the size of the data packet and energy efficiency and showed that FEC improved energy conservation whilst retransmissions caused energy inefficiency. The proposal introduced additional parity bits and an increased energy consumption through encoding and decoding.

#### (i) SensorMAC (SMAC) Protocol

The SensorMAC (SMAC) protocol employed a duty cycle that is synchronised and a planned intermittent wake and sleep cycle [29]. It used a short SYNC packet that periodically exchanged sleep schedules with immediate neighbouring sensors. SMAC reduced energy waste through decreasing idle listening by predefining sleep and listen periods but fell short when the node sat between two awake clusters, as it would have to follow two distinctive schedules that would result in more energy consumption. The SMAC had static sleep–listen

periods which cause high latency and lower throughput. These sleep schedules decreased the energy utilisation triggered by idle listening. The overhead of time synchronisation could be reduced by announcing sleep schedules. The disadvantage was an upsurge in the probability of collision because broadcast data frames did not utilise RTS/CTS. When the traffic load was variable, the efficiency of SMAC decreased because of the sleeping and listening periods being prescribed and constant. SMAC typically had low throughput and high latency.

(ii) Timeout-MAC (TMAC) Protocol

Timeout-MAC (TMAC) [30], is an adjustable energy efficient medium access control protocol used in wireless sensor networks which reduced idle listening meanwhile taking into consideration the hardware restrictions and the wireless communication configurations. TMAC introduced an adaptive duty cycle by ending the active section of its sleep-sense cycle dynamically. This resulted in reduction in the energy consumed by idle listening, wherein the sensor nodes potentially linger, waiting for messages to come in whilst still maintaining a realistic throughput. When there was no activation event for a particular time limit, the listen period ended. The node that was in its active period would send or receive data, but that active period would end if there was no action for a specified time. In WSNs, variable loads were anticipated, considering the fact that sensor nodes which are located close to the sink should convey more traffic, which might vary over time. While TMAC produced a superior outcome under varying loads compared to SMAC, it broke the synchronisation of the listening periods inside the virtual clusters. Disrupting the synchronisation caused the early sleeping problem where a third node meant to be part of the next transmission process went to sleep and this severely affected throughput.

(iii) Sift Protocol

In the case of a shared medium, there is contention to transmit simultaneously on the channel when more than one sensor node senses an event. Sift is a medium access control protocol for WSNs designed to deal with many sensors in a shared medium attempting to transmit at the same time. It was developed for sensor network environments that are event driven that minimise the amount of time it takes to send a number ( $x$ ) of these messages without collisions [31]. Sift performs well when geometrically-linked contention occurs and adapts well to sudden changes in the number of sensors ( $y$ ) that are trying to send data. The number of sensors with a message to send is always less than or equal to the number of sensor nodes with data to send. The rest of the sensor nodes suppress their transmissions. When sensing of an event occurs, it is

adequate that whichever  $x$  of  $y$  sensors that senses an event should report it with low latency. Sift used a geometrically-expanding probability distribution inside a contention window whose size was fixed as opposed to numerous conventional MAC protocols whose contention window size is variable. Sift had a disadvantage of increasing the idle listening brought about by listening to all the slots before transmitting. The other disadvantage was overhearing, whereby if transmission was in progress, sensor nodes would listen until the end of the slot in order to compete for the next transmission slot.

(iv) WiseMAC Protocol

The WiseMAC protocol is centred on a carrier sense multiple access scheme and employed the dynamic preamble sampling method to curtail the energy spent while listening to an idle medium [32]. This protocol is unique in that it exploited the knowledge of the sampling schedule from the direct neighbours of the sensor and created a wakeup preamble of a much smaller size. WiseMAC did not require setup signalling or synchronisation of the whole network and adapts to the traffic load. It provided very low power consumption in conditions of low traffic and high energy efficiency when the traffic conditions were high. This scheme permitted a reduction in the transmit and receive mode energy consumption and wasted energy due to overhearing. Additionally, protocol definition handled clock drifts, mitigating the requirement for external time synchronisation. The key disadvantage was that the distributed listen-sleep scheduling caused diverse sleep and wakeup times for every node neighbour. This resulted in redundant transmission which would cause greater latency and more energy consumption.

(v) Traffic Adaptive MAC Protocol

The TRAMA, a channel access protocol is collision free and energy efficient and known as Traffic Adaptive MAC protocol was proposed in [33]. It allowed sensor nodes to adopt a low power idle state whenever there was no transmission or reception of data packets, hence ensuring that there were no collisions during unicast or broadcast transmissions thereby decreasing energy consumption. TRAMA assumed that time is slotted and employed a distributed selection system built on traffic information at every sensor node to establish which node needed to transmit at a specific time slot. Using traffic information, TRAMA allowed the nodes to decide when they could shift to the idle mode and not listen to the channel and prevented allocating time slots to nodes that did not have any traffic to send. This meant that any node that was idle was not an intended receiver and therefore did not experience any

receiver collisions. TRAMA achieved less probability of collision and greater percentage of sleep time in comparison with CSMA based protocols. The disadvantage of TRAMA is the high latency due to the higher duty cycle.

(vi) Berkeley-MAC (BMAC) Protocol

Berkeley-MAC (BMAC) was presented in [34] as a protocol for low power wireless sensor networks. The protocol used Clear Channel Assessment (CCA) and an optimisation approach called Low Power Listening (LPL). This approach introduced duty cycle to curb idle listening. LPL extended the length of the preamble in the data packet so that receivers could periodically search the channel. Because the listening intervals were long, it made the LPL-based protocols energy inefficient, since time required for the preamble signal transmission was relative to the channel listening interval.

### 2.3.3 Cross Layer Optimisation

Several proposals of cross-layer optimisation have been put forward in literatures considering different technologies, protocols and schemes [35, 36, 37]. Cross-layer optimisation shares information between different layers of the protocol stack and exploits the inter-layer dependence. It becomes vital to compare the efficiency of the several protocols to establish which approaches result in better network performance. Cross-layer design requires that the parameters of two or more layers be recovered and altered to accomplish the optimisation objective [37]. Most of the cross-layer optimisation techniques in the reviewed literature involve the MAC layer and physical layer [38]. Since every layer of the protocol stack contains a characteristic interconnection with other layers, cross-layer schemes can improve energy efficiency significantly through adaptive transmission and resource allocation techniques that correspond to the dynamics of traffic, service and the environment. In wireless sensor networks, the typical objectives of cross-layer optimisation are minimisation of energy utilisation [38], optimal scheduling [39], efficient routing [40], topology control [41] and QoS provisioning [42].

(i) Energy Constrained Path Selection (ECPS) Protocol

Energy Constrained Path Selection (ECPS) technique as well as Energy Efficient Load Assignment (E2LA) were put forward by [43]. ECPS employs cross-layer interfaces involving the network layer and the MAC sub layer. The major goal of the ECPS was to maximise the likelihood of transporting a data packet to its destination in a specified maximum number of

transmissions. ECPS exploited probabilistic dynamic programming techniques that allocated a unit reward if the favourable event occurred, that is, getting to the destination in the number of required transmissions or less, and allocating no rewards if otherwise. Maximising the projected reward corresponds to the likelihood that the data packet will reach its destination in a set number of transmissions being maximised. This approach achieved the objective but had no ways of using numerous routes concurrently. E2LA was then used to counter the problem of ECPS not being able to simultaneously use multiple routes to transmit. E2LA distributed the routing load among an array of energy aware routes. It assigned routing loads in accordance with the following four distinct reward schemes,

- a) Boolean Reward: if a data packet was successfully transported to its destination without encountering any errors a unit reward was allocated, otherwise the reward equaled zero.
- b) Signed-Unity Reward: if a data packet was transmitted successfully with no error encounters, a unit reward was allocated, otherwise the reward equaled minus unity.
- c) Contention Indicator ( $CI_R$ ): a number for a particular route showing the probability of transmission failure largely due to the competition for the medium access.
- d) Basic Contention Resolution Based Reward (CRB): if a signed unity reward was allocated and a negative reward assigned to a particular route considering the number of packets that need to be delivered as well as  $CI_R$ .

(ii) Cross-Layer MAC (MAC-CROSS) Protocol

Cross-layer MAC protocol called MAC-CROSS which is energy efficient, is employed in [44]. This protocol utilised information on routing found at the network layer on the MAC layer so that it can maximise the sleep interval of individual nodes. The MAC-CROSS protocol addressed the compulsory wake-up problem caused by periodic listen/sleep-based approaches. It minimised energy depletion by continually switching OFF the radio interference of redundant nodes that are not encompassed in the routing path. Depending on the state defined by data transmission, the nodes were categorised into three distinctive groups:

- a) Communication Parties (CP) which denoted each node presently taking part in the transmission of data.
- b) Upcoming Communicating Parties (UP) which denoted every node that would be included in the actual transmission of data.
- c) Third Parties (TP) referring to every node that was not involved in a routing path and therefore not at all included in the actual data transmission.

(iii) Transmission Scheme Optimisation Protocol

In the cross-layer scheme proposed in [45], the authors considered a cross-layer architecture encompassing the data link layer, the medium access control layer and the routing layer. The authors based their model on the energy consumption in the transmitter circuit and in the data transmission. They used their model to maximise the network lifetime by optimising the transmission schemes. The authors sequentially optimised a single layer at a time, whilst holding the other two layers constant. Their objective was to choose the rate of transmission for every link that minimises the consumption of power while maximising the lifetime of the network. They managed to solve the optimisation problem precisely for TDMA networks, but for other networks with interference, they proposed approximation techniques to resolve the optimisation challenges.

(iv) Joint Routing, MAC and Link Layer Optimisation Protocol

In the work of other researchers, the emphasis is on the fact that every layer of the protocol stack must support energy efficiency across all layers using cross-layer design [46]. The authors analysed joint routing that is energy-efficient, link adaptation strategies and scheduling that maximise the network lifetime. The authors proposed TDMA strategies of variable length where the routing requirements determined the slot length which minimised the consumption of energy throughout the network. The results showed that joint design of MAC layer and routing layer conserved more energy compared to the traditional designs. They also showed that link adaptation improved energy efficiency by reducing transmission time using higher constellation sizes, thereby reducing the extra circuit energy consumption. Multi-hop routing was found to be more energy efficient than single-hop routing using link adaptation. The authors did not propose a communication protocol for practical implementation and their approach did not consider congestion and flow control in the transport layer.

(v) Unified Cross-Layer (XLP) Protocol

In [47] the authors combined the processes of the conventional communication layers into a single protocol that had reliable communication with minimum energy utilisation, local congestion avoidance and adaptive communication decisions. Analysis and evaluation of the performance and results of the simulation experiment showed that XLP significantly improved the communication operation. It eclipsed the conventional protocol layer scheme regarding both the complexity of implementation and the network performance. This approach

investigated communication of this single protocol but did not take into consideration the other functionalities such as error control, topology control and modulation.

(vi) Energy Optimisation Approach (EOA) Protocol

A proposition to optimise the physical layer, medium access control layer and the network layer, was put forward in [48] known as the Energy Optimisation Approach (EOA). The focus was on computing the transmission power, duty-cycle and routing schedule that optimise the network's energy efficiency. The EOA dynamically regulated the transmission power in the physical layer until it achieves an appropriate power level between the nodes. Concurrently, every node managed a neighbour table to register this appropriate transmission power level. Every node utilised the neighbour table in the physical layer to construct its routing table in the network layer. The EOA then employed the routing information from the table to establish each node's duty cycle while, EOA used the cross-layer routing information to determine the duty-cycle of each node, while paying attention to the overhearing problem and collisions in the MAC layer. The results showed that more energy was conserved due to EOA.

(vii) PHY and MAC Layer Optimisation Protocol

Another cross-layer approach of optimising the lower layers of the protocol stack was developed in [49]. They focused on the physical layer and the medium access control layers. They developed a cross-layer analytical technique which employed a Markov chain model which brought into consideration the success probability for new packet arrivals, channel access and packet transmission. They realized that lower layers of the protocol stack that are jointly optimised would produce efficient communication channel for the upper layers resulting in energy conservation.

More recent studies are focusing on efficient energy use in wireless sensor networks in relation to the environment. Energy harvesting technology is a technique with the ability to extract energy from a sensor node's ambient environment. It potentially solves the problem of energy efficiency in WSNs. The ability to harvest energy from the surrounding environment facilitates the achievement of an infinite lifetime in a sensor node. This technology revolutionises the underlying theory of communication protocols in WSNs. Rather than conserving as much energy as possible, the protocols guarantee the energy being harvested is equivalent or greater than the energy being consumed, thus keeping the operation efficient and maximising on network performance.

(viii) ERI-MAC Protocol

A novel MAC protocol for harvesting energy in sensor networks which is receiver initiated and known as ERI-MAC was proposed in [50]. Rather than focus on the aspect of saving power, the purpose of this protocol is to harvest energy under certain conditions and use it to improve network performance and increase network lifetime. Unlike the conventional MAC protocols, ERI-MAC achieved infinite network lifetime by maintaining the sensor nodes operating at a state called the Energy Neutral Operation (ENO). In the ENO state, the energy consumption of a sensor node is constantly lower than or equivalent to the harvested energy from the environment. Additionally, wireless sensor networks that are capable of harvesting energy assume the interdependency between energy harvesting and performance. ENO-Max is a state reached by a sensor node when it is operating at its maximum performance while in the ENO state. When using ERI-MAC the mechanism of queuing packets is implemented to adjust the sensor node operation to the rate of harvested energy. If the ratio between the energy consumption in the sensor nodes and the harvested energy in the network is greater than one, the nodes shift to the sleep mode and stay there until the batteries have stored enough energy to the required levels. The simulation results of this study showed that infinite lifetime could be achieved by keeping all the sensor nodes in the ENO state, thus providing good performance.

(ix) Energy Harvesting (EH) Protocol

This emerging green alternative was also developed in [51], where energy harvesting (EH) was optimised for the PHY and MAC layer. The authors first studied the optimisation of the physical layer of a single link scenario in which a transmitter communicates with a receiver. They investigated two different cases:

- a) In the first case, the EH transmitter had no channel state information and used retransmissions to increase the reliability of communication; the goal was to optimise the EH node's transmit power settings.
- b) In the second case, the EH transmitter had channel state information and could adjust its transmit power as a function of channel state. Furthermore, the system design explicitly incorporated storage inefficiencies and the different timescales at which the energy harvesting and fading processes evolved.

The authors then considered energy-efficient multi-hop communication using multiple EH cooperative relay nodes that transmitted over a common channel. The system brought out the inter-relationship between several aspects related to cross-layer system design for EH nodes.

Examples are, multiple access layer design, amplify-and-forward cooperative relaying to exploit spatial diversity, to improve robustness to fading, and two-hop communication to improve energy efficiency. While energy conservation and spectral-efficiency maximization continue to remain desirable design objectives for WSNs, they become secondary goals in energy harvesting. The primary design focus changes to prudently using all the harvested energy and ensuring its availability for consumption when required. Being too conservative in consuming the harvested energy simply wastes the harvested energy, while being too aggressive leads to the node unnecessarily being starved of the energy it requires at later time instants. Crucial factors that ought to be considered in the design are, the profile for energy harvesting, the ability to store energy and the availability of channel information or its non-availability.

Joint functionality potentials of the PHY and MAC layers to enhance energy efficiency in wireless sensor networks were identified in [52]. The study decoupled and investigated the fundamental factors of the two layers that correlate and generally have an impact on energy conservation, namely Adaptive Modulation and Coding (AMC), fading models, scheduling gain and throughput. They demonstrated the combined effect of these parameters on the basic functions of the network. They presented aspects of energy efficiency on the physical layer regarding link adaptation. When AMC was linked with OFDMA diversity technique, it provided an AMC function that is energy efficient. The study investigated the effect of multipath fading models such as Nakagami-m and Rayleigh on average link energy efficiency. It demonstrated the possibility of maximising energy conservation using link adaptation.

Analytical and simulation models have been used in the evaluation of the performance of different medium access control protocols. In [53], the author propositioned a Markov model that analyses saturation throughput with ideal channel conditions of IEEE 802.11 having finite stations that always have a packet to transmit but with infinite retransmissions. The study in [54] provided a Markov model that evaluated the performance of a single-hop network using SMAC, analysing network throughput, packet service delay and energy consumption. The model, however, did not consider packet queueing delay which is essential in determining packet latency. Some work focused on the analysis of specific metrics for a particular MAC protocol or a string of them that have similar characteristics, such as the work presented in [55]. They analysed the distribution of end-to-end delay in a wireless sensor network using a Markov process. Many researchers have analysed the behaviour and performance of PHY and MAC

layers using FEC [56-62] and stochastic techniques respectively [63,64]. Although these studies analysed the behaviour and performance of optimising the layers, most of the studies do not quantify the gains achieved.

#### 2.4 Proposed Solution

This research defined and implemented a mathematical model for the 802.11g (Wi-Fi) to evaluate the impact of cross layer optimisation on energy consumption and throughput. The PHY layer and MAC layer were tuned to improve communication performance in a wireless temperature sensor network. The PHY layer was optimised by the introduction of forward error correction in the form of Reed Solomon code. The energy consumption performance was evaluated for a range of code rates. S-Aloha was used as the medium access protocol and a non-contention MAC protocol SMAC was also used to compare energy efficiency between the two protocols. This allowed for the determination of practical synchronised transmissions under different MAC schemes. The medium access control protocol employed is S-Aloha because of its low communication overhead and ease of implementation. MATLAB was employed as the simulation platform [65,66].

This proposed solution differs from the reviewed existing solutions in that the proposed mathematical model accurately describes contention at the MAC layer, which is not apparent in the existing solutions. The proposed solution also evaluated and quantified the energy gains achieved by the cross-layer optimisation of PHY and MAC layer and produced expected results which are reflective of more realistic parameter considerations.

#### 2.5 Chapter Conclusion

This chapter reviewed several schemes that have been used to conserve energy through optimising the protocol stack. Focus was placed on optimisation of PHY and MAC layers as individual layers. Different types of cross-layer protocols and their approach to energy conservation were presented. The focus on cross-layer optimisation was jointly optimising the functionalities at the different layers of the protocol stack to minimise energy consumption thus maximising the network lifetime. Although the schemes reviewed in this chapter result in energy conservation, most of them do not quantify the gains achieved. This study quantifies the gains in energy consumption that can be obtained by applying the Markov chain model [67,68,69]. The next chapter outlines the proposed solution.

## CHAPTER THREE: ANALYSIS OF THE PROPOSED SOLUTION

### 3.1 Introduction

In the previous chapter a review of literature on conservation of energy using layers of the protocol stack in WSNs was conducted. A gap in quantifying actual gains that could be obtained by cross-layer optimisation was found. This chapter outlines the proposed solution and decomposes it into several constituent parts. The purpose of this study was to investigate an energy consumption model by jointly tuning the PHY and MAC layers of a Wireless Temperature Sensor Network to design and implement a mechanism that would provide or result in energy savings in WTSNs.

### 3.2 Proposed Solution

The PHY layer and MAC layer were tuned to improve communication performance in a wireless temperature sensor network. The PHY layer was optimised by the introduction of forward error correction in the form of Reed Solomon code. The energy consumption performance was evaluated for a range of code rates. The medium access control protocol employed is S-Aloha because of its low communication overhead and ease of implementation.

The probability of packet collision when accessing the channel was employed to tune the MAC layer. A contention-free MAC protocol, SMAC, was also used to compare energy consumption between the two MAC protocols. The proposed mathematical model accurately describes contention at the MAC layer. This allowed for the determination of practical synchronised transmissions under different MAC schemes. Potential energy gains were determined for different RS codes considering the probability of channel access. The research evaluated the average number of steps required by a sensor node to successfully transmit a data packet during a transmission period using a Markov chain model. The model facilitated the determination of the number of steps required for every sensor node to have reported its observation to the sink node successfully. When the length of every step is known, the number of steps to absorption can be converted into time to absorption. Knowledge of the time to absorption facilitated for the analysis of the consequence of tweaking the parameters of the protocol stack.

### 3.3 Components of the proposed solution

The proposed solution centres around components shown in Figure 1. The objective of the research was to improve communication performance, and thus, the function of each component of the communication system is described as follows:

- (i) Sensors: Senses the environment and produces a message signal.
- (ii) Source Encoder: Converts message signal into a series of binary digits.
- (iii) Channel Encoder: Aims to render the transmitted signal resistant to interference and noise by adding redundant information for error recognition and correction.
- (iv) Modulator: Maps the binary digits into signal waveforms.
- (v) Channel: Provides the communication between the transmitter and the receiver.
- (vi) Demodulator: Processes the transmitted waveforms that have been corrupted by the channel and condenses each waveform to a data symbol.
- (vii) Channel Decoder: Corrects the errors in the signal.
- (viii) Source Decoder: Decodes the series from the information in the encoding process which produces an approximate copy of the input signal.
- (ix) Information Sink: Receives the message signal sent by the nodes.

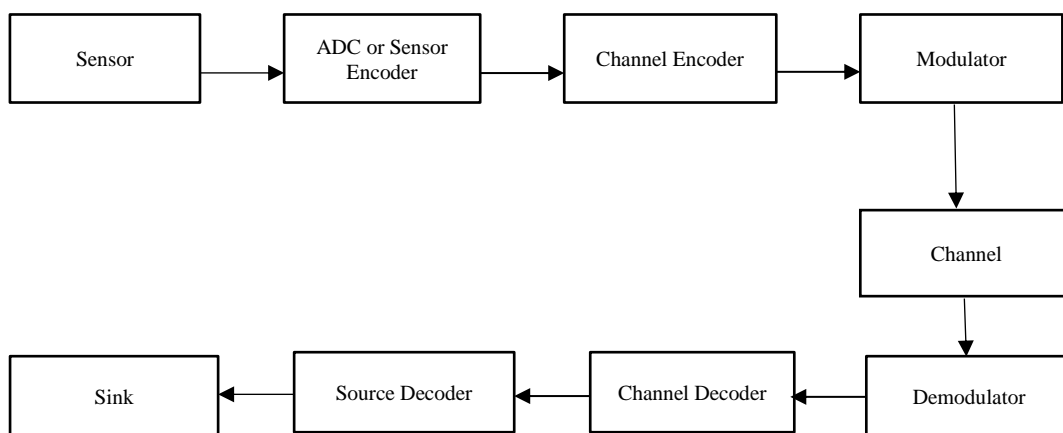


Figure 1: Communication Block Diagram

### 3.4 Function of the components of the communication system

The sensor nodes detect and collect temperature data from the environment. A wireless sensor node consists of four subsystems in its architecture, namely, the communication subsystem which enables wireless communication, the computing subsystem allows data processing and the administration of node operation, the sensing subsystem, which links the wireless sensor node to cyberspace and finally the power subsystem which provides the system supply voltage.

[1] The architecture of the wireless sensor node is shown in Figure 2.

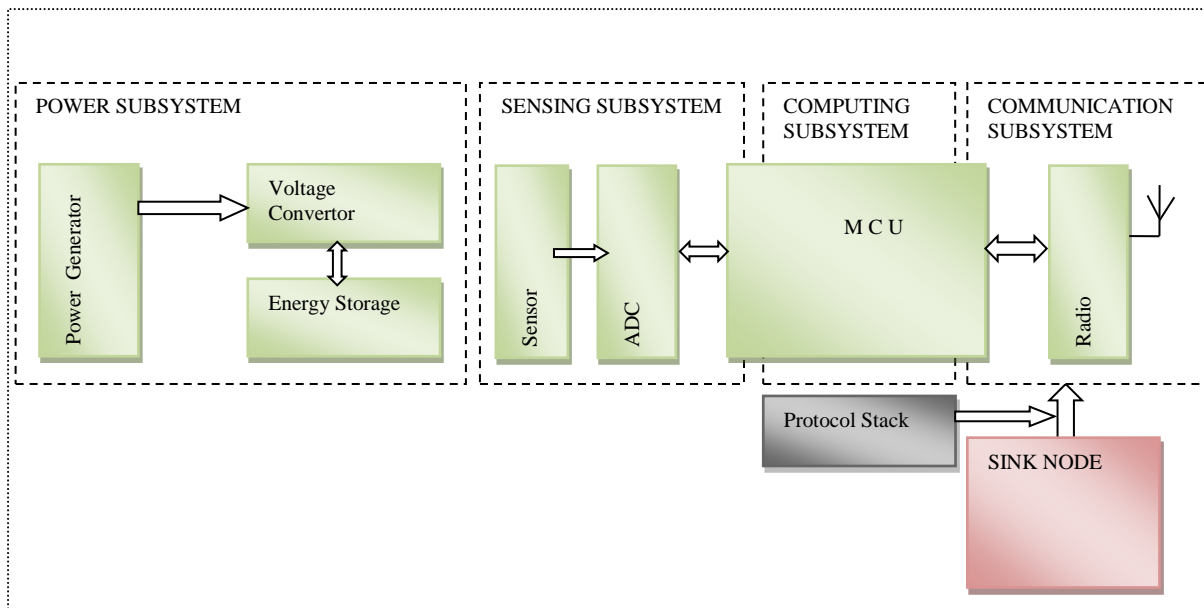


Figure 2: Wireless sensor node architecture [1]

The message signal, which is the temperature sensed by the sensors, is converted to a stream of binary digits in a process known as source encoding. Employing a source-coding technique which is energy efficient is vital so that the channel bandwidth and signal power requirements are met. The source-coding process entails sampling, quantizing, and encoding to convert the analog signal to digital form. The analog signal is discretised in time intervals to become a discrete signal. This discrete signal then goes through amplitude discretisation resulting in a digital signal. The source encoder ultimately encodes this digital signal to binary digits. The series of binary digits is transferred to the channel encoder, where redundancy is introduced to subdue errors and mitigate against noise and interference. It is also known as error control coding. The channel encoder adds bits to the message bits that need to be transmitted methodically. The additional redundancy aids in increasing the dependability of the data received and enhances the reliability of the received signal. The channel decoder output is routed to the digital modulator which functions as the link to the communication channel.

Modulation is a process which involves altering the frequency, amplitude and phase of a carrier signal according to the message signal. It largely involves converting a baseband message signal to a passband signal at a considerably higher frequency. Modulation results in the message signal becoming robust to noise, the channel capacity being utilized efficiently, and the signal detection simplified. The series of binary digits from the channel encoder is mapped into signal waveforms. A modulator that is power efficient allows the communication system to consistently broadcast data at the smallest practicable power cost. A modulator that has

spectral efficiency allows the communication subsystem to transmit as many binary digits as possible within a restricted frequency range. There is a trade-off between the two because it is not possible to obtain power and spectrum efficiency simultaneously.

To transfer the information signal from the transmitter to the receiver, a physical medium is employed called the channel. In the case of wireless communication, the channel is the atmosphere. In the channel, signal distortion occurs, being caused by additive noise. This noise can result from atmospheric noise or interference from other channel users in the same spectrum. To mitigate against noise, the signal to noise ratio is made considerably large so that the channel becomes oblivious to noise, or the spread spectrum technique can be employed to distribute the transmitted signal's energy to achieve a wider effective bandwidth. The demodulator extracts the baseband message signal from the channel to facilitate its processing and interpretation by the intended receiver.

Demodulation recovers the original signal coming from the sender end in modulated form and reduces it to a data symbol. The function of a demodulator is opposite to that of the modulation process. The channel decoder undertakes to rebuild the sequence of the original information from the knowledge of the channel encoder's code and the redundancy enclosed in the received data and corrects the errors in the signal. The source decoder has the knowledge of the method used in source coding, receives the output bit stream from the channel decoder and tries to rebuild the original signal from the signal source. Owing to errors in channel decoding and probable distortion brought in by the source encoder, the signal at the output of the source decoder approximates the original message signal. The degree of the distortion imported by the communication system is given by the variance between the original signal and the restructured signal [10].

### 3.5 Optimising Physical and MAC Layers

Figure 3 presents an optimisation block diagram for the proposed solution. The research explores the possible energy gains that could be accomplished by optimising the forward error correction rate (FEC). FEC is a process of attaining error control in the transmission of data where the transmitter (source) sends redundant data and the receiver (destination) identifies just the section of the data that comprises no evident errors. FEC codes can detect and rectify a restricted number of errors without having to retransmit the data bits. The two elementary types of FEC codes are the convolution codes and the block codes [53]. For the purposes of

this research, block codes will be used, in the form of a fixed Reed Solomon (RS) code. It was preferred because of its strong error correction capabilities and mitigates against latency.

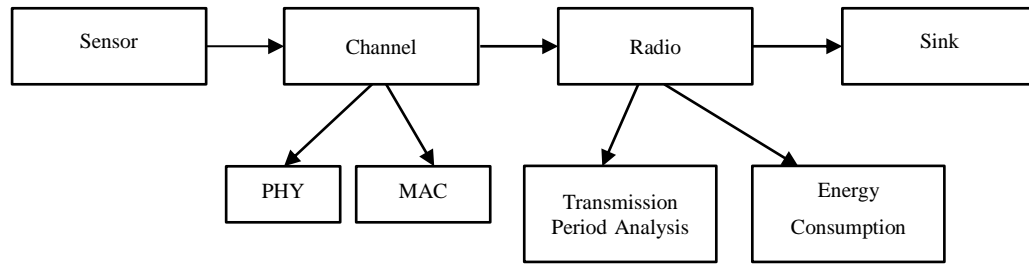


Figure 3: Optimisation Block Diagram

At the physical layer level many methods can be applied to enhance the performance of the PHY layer, namely power control, modulation, error control coding and source coding, whereas at the MAC layer there are design challenges such as overhearing, idle listening, packet collision avoidance, and control overhead minimisation that need to be resolved efficiently. In this research, a study of the potential energy savings obtained using the ECC approach, was undertaken, considering the probability of packet collision during the channel access competition period. The possible energy gains were investigated for varied error correction code rates. The minimisation of the control overhead in the MAC layer was circumvented by selecting a basic SMAC and S-Aloha protocol and a performance comparison done between the two protocols.

### 3.6 Wireless Sensor Network

Wireless sensor networks are a collection of sensor nodes that form a wireless link between them. The sensor nodes are distributed in an environment where they gather information and forward it to the sink node. Sensor nodes not only communicate with the sink node or base station, but also with each other by means of their wireless radios, permitting them to broadcast their sensed information for remote processing and analysis. There are different topologies employed to set up wireless networks, namely star, ring, bus, mesh and cluster and hierarchical. The selection of the network topology hinges on the volume and the rate of occurrence of the data to be transmitted, the distance for transmission, whether the sensor nodes are mobile and battery life requirements. Figure 4 shows a star topology which is employed in this study. In a star topology, the wireless sensor nodes are within direct communication range to the sink node, about 30-100metres. It has the lowest power consumption overall, compared to other topologies although limited by the radio transmission distance.

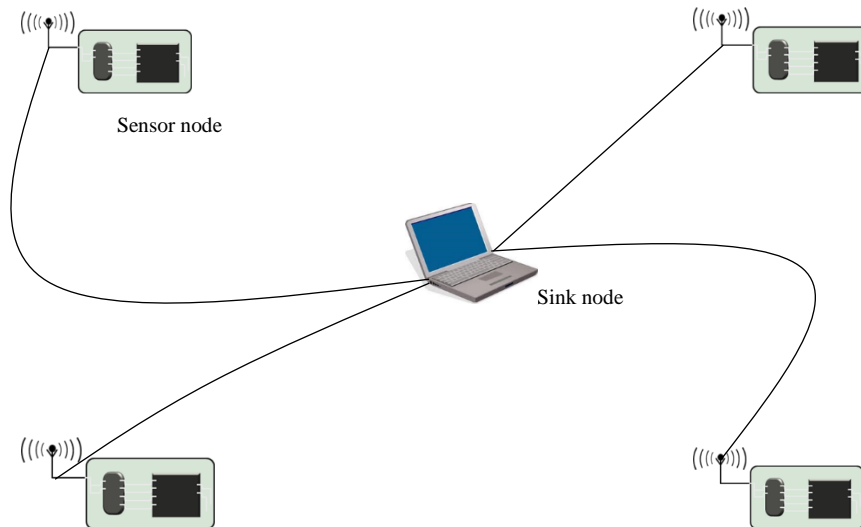


Figure 4: Star Topology Network [1]

### 3.7 The 802.11g channel

Electromagnetic waves are used to transmit data between devices in 802.11 wireless networks and are therefore prone to interference. From the wide spectrum of electromagnetic waves available, 802.11 uses radio waves with a specific frequency. The radio bandwidth consists of licensed and unlicensed bands which are available for use. The licensed bands are subject to regulation to circumvent undesirable interference between different users and systems of the bandwidth. Users of these frequencies need to apply for a license, for example, broadcast license or WiMax license. 802.11 networks employ the 2.4GHz unlicensed bandwidth, namely, the Industrial, Scientific, and Medical (ISM) bands. Employing an unlicensed band implies that individuals can just purchase equipment and start to transmit data without seeking any permission from the government or frequency allocation body. However, the ISM bands are dogged with interference from cordless phones, microwave ovens, Bluetooth devices etc., because there are no usage restrictions. Figure 5 shows where, in the electromagnetic spectrum, the unlicensed frequency bands used for wireless networks reside.

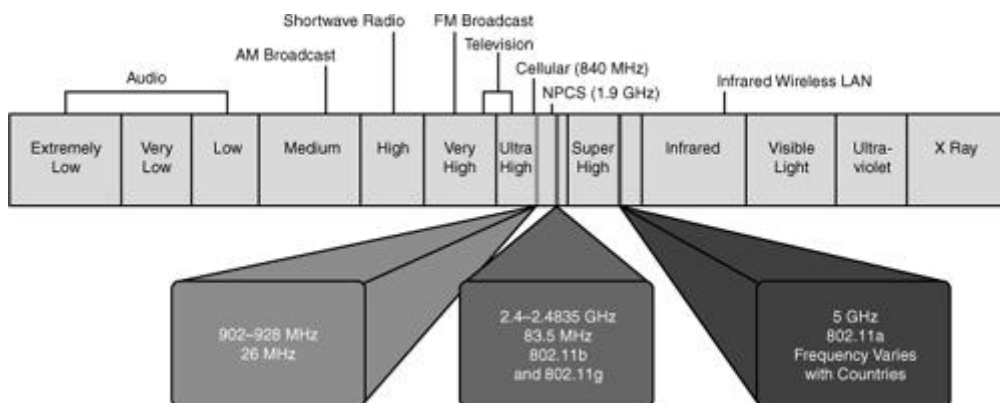


Figure 5: Unlicensed frequency bands [1]

Protocols have been established and approved by the Institute of Electrical and Electronic Engineers (IEEE) that guide manufacturers to build devices that communicate with each other. These protocols prescribe the data rates, modulation and frequency bands used, among other things. The protocols for 802.11g are covered in [19] in detail. According to these protocols, the maximum data throughput for 802.11g is 54Mbps, while the maximum transmit power permissible is 100mW. The 2.4Ghz frequency band is divided into channels 22Mhz wide. All the channels overlap except three. The 802.11g protocol employs two forms of modulation schemes, namely, Direct Sequence Spread Spectrum (DSSS) as well as Orthogonal Frequency Division Multiplexing (OFDM). DSSS is available for backward compatibility with earlier 802.11b devices.

The OFDM modulation technique works as follows: it splits available bandwidth into equally spread out frequency bands. Each band, a high-speed data carrier, is split into numerous low speed subcarriers that carry a portion of the user information which are then transmitted in parallel. Each high-speed data carrier is 20MHz in width and is divided into fifty-two subcarriers that are about 300KHz wide. Forty-eight of these fifty-two subchannels are used for data, while the four remaining ones are used for error correction. BPSK encodes 125kbps of data per channel, resulting in 6Mbps data rate [10].

### 3.8 Physical layer

The physical layer is responsible for the transmission of data. It outlines the electrical and physical specifications for devices, thus principally defining the interdependence between a device and a communication medium. The main operations and services executed by the physical layer are, establishing and terminating a connection to the medium of transmission, effectively sharing communication resources amongst several nodes. An example of some of the functions and services are flow control and contention resolution, modulation of digital data at the sensor nodes and the corresponding signal transmitted over the radio link in the communication channel. The physical layer is partitioned into three sublayers, as shown in Figure 6. The Physical Layer Convergence Procedure (PLCP) sublayer is responsible for assembling packets for different physical layer techniques as well as the Clear Channel Assessment (CCA) mode, a carrier sense mechanism which determines whether the medium is idle or not. The Physical Medium Dependent (PMD) layer stipulates the modulation and coding techniques. The Physical Layer Management Entity (PLME), is concerned with managing

matters such as channel tuning and coordinates the interaction between the PHY and MAC layers [19].

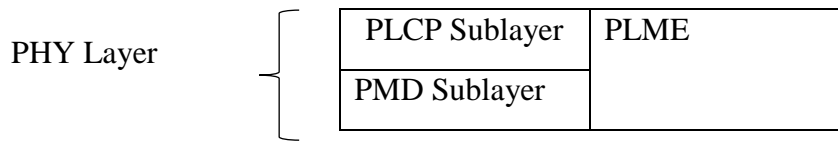


Figure 6: Structure of the Physical Layer

The 802.11 physical layer utilises burst broadcasts or packets. Each packet consists of a preamble, a header and payload data as shown in Figure 7. The preamble is responsible for timing and frequency synchronisation at the receiver. It ensures that transceivers correctly interpret the start of data transmission using a sequence of bits. The header specifies information about the configuration of the packet for instance packet size, data rates, destination address etc. The payload data is the actual data from the user that the packet is transporting. The 802.11 standards define the types of frames used in data transmission and for managing and controlling wireless links. These frames types are divided into three functions, data frames, control frames and management frames [19].

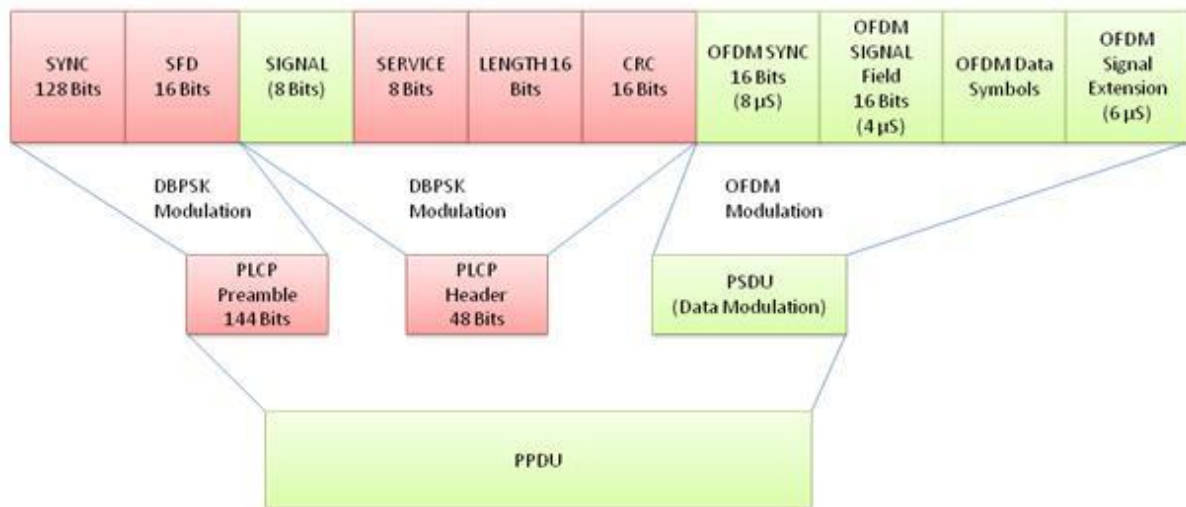


Figure 7: 802.11 packet format [19]

### 3.8.1 Error Control Coding

In wireless communication, whether it is radio broadcasting, cell phone communication or Internet connection, it is essential that data is decoded error free across the wireless medium. When a channel is affected by Gaussian noise, there is a limit that defines the maximum channel capacity or the possible error free transmission rate for a given signal to noise ratio

and channel bandwidth. The challenge is that channel noise could cause errors in the data during transmission. To overcome this challenge, forward error correcting codes are applied to identify and correct these possible errors at the receiver. Error control coding involves procedures of ensuring delivery of data from a transmitter to a receiver with the least amount of errors. It reduces the effects of noise in the channel during transmission of data, which causes the errors, by allowing the receiver to rebuild corrupted bits without the need for retransmission.

Any desired level of error rate can be determined and incorporated in the system. Error control can be achieved by incorporating redundant bits into transmitted data, resulting in the transmitted data having more bits in the bit sequence than that of the original information being represented. Forward error correction is a type of error control coding that is used in this research. FEC method inserts redundancy to the original data in the form of parity bits, and typically, the more the parity bits generated, the more possible errors could be identified and amended. Different forward error correcting types can be used, for example, the main types are block codes or convolution codes. Block codes use fixed length blocks of bits to a predetermined size, while convolution codes work on bit streams which have arbitrary length.

Figure 8 shows that data bits presented to the encoder are segmented into equal length blocks of  $b$  binary digits and the data mapper maps each  $b$ -bit message block into an  $n$ -bit code word, where  $n$  is greater than  $b$  because of the added redundancy bits. The symbol length “ $b$ ” represents the number of bits per symbol, and “ $n$ ” is the block length given as  $n = 2^b - 1$ , symbols. The decoder has the task of determining if there has been an error by comparing the received sequence with the transmitted codewords. Every error correction code has three fundamental features, namely, code length, code dimension and the minimum distance. The code length,  $n$ , relates to the number of symbols per codeword. The code dimension,  $k$ , relates to the number of data symbols transmitted in one codeword. The minimum distance,  $d_{\min}$ , refers to the minimum number of symbol differences between code words.

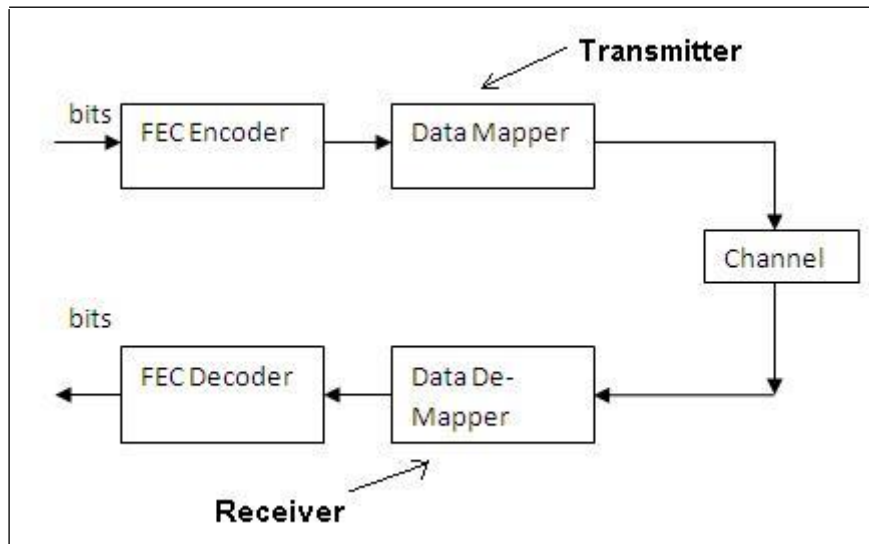


Figure 8: Forward Error Correction Scheme

The FEC scheme influences the bit error rate in data transmission. A theoretical expression to find bit error probability can be derived in relation to energy per received bit versus the single sided noise power spectral density,  $E_r/N_o$  on the AWGN channel. The same will be done for systems that employ coding, in this case, Reed Solomon codes. However, the problem of comparability must be resolved because error coding creates additional bits, and this results in increasing the time it takes to send a data packet or to increase the bandwidth, so that transmission can be faster. Whichever circumstance, the overall noise in the message will increase; primarily due to noise from the channel for an extended period and secondly because more noise falls within the frequency range [70].

The ratio of energy per bit of information to noise power is used to assess the error performance of the communication link. Consequently, when coding is applied, the number of information bits would be less than the transmitted bits since the packet length is fixed, resulting in an increase in  $E_b/N_o$  in relation to  $E_r/N_o$ . The redundancy is given a quantitative measure known as the coding rate,  $R$ , which is defined as the ratio of the message length to the codeword length. As an example, if a codeword of length  $n$  is generated from a message of length  $k$ , then the coding rate  $R = k/n$ . The maximum value the code rate can achieve is one, which occurs when no coding is applied, and the message is uncoded. Coding performance and coding rate are two contrasting aspects. As more redundant bits are added, it strengthens the error correction capability while the coding rate declines. An excellent code maximises the error correction performance while maintaining the coding rate close to one.

### 3.8.2 Reed Solomon Codes

As previously mentioned, there are primarily two types of FEC coding techniques, the linear block coding and convolution coding. The Reed-Solomon (RS) codes used in this research fall under linear block codes. RS codes are a special class of non-binary BCH codes. They differ from binary BCH codes given that non-binary BCH codewords comprise of symbols over GF( $2^b$ ) ( $b \geq 2$ ), (Galois Fields), whereas binary codewords consist of binary digits of ones and zeros. As a result, arithmetic processes in non-binary BCH codes are no longer straightforward XORs and ANDs but are executed over Galois Fields ( $2^b$ ). Save for that, all the characteristics related to binary BCH codes apply equally to non-binary codes. Equation (1) is the cyclic code generator, commonly known as the generator polynomial [70].

$$g(X) = g_0 + g_1X + g_2X^2 + \dots + g_{2t-1}X^{2t-1} + g_{2t}X^{2t} \\ = (X + \alpha^1)(X + \alpha^2) \dots (X + \alpha^{2t}). \quad (1)$$

where  $\alpha$  is a primitive element of GF( $2^b$ ) and  $\alpha^1, \alpha^2, \dots, \alpha^{2t}$  are elements of the same field.

Since  $g(X)$  is of degree precisely  $2t$ , all  $(n,k)$  RS codes satisfy the following equation:

$$n - k = 2t. \quad (2)$$

By design, the Reed-Solomon code can correct up to  $t = (n - k)/2$  errors. The decoding decision system employed is the hard decision decoding where the demodulator quantises the inbound signal into two states symbolised by zero and one. The data stream bits are then recovered by the decoder that would have a specific error correcting capability. Figure 9 shows how the symbols are structured.

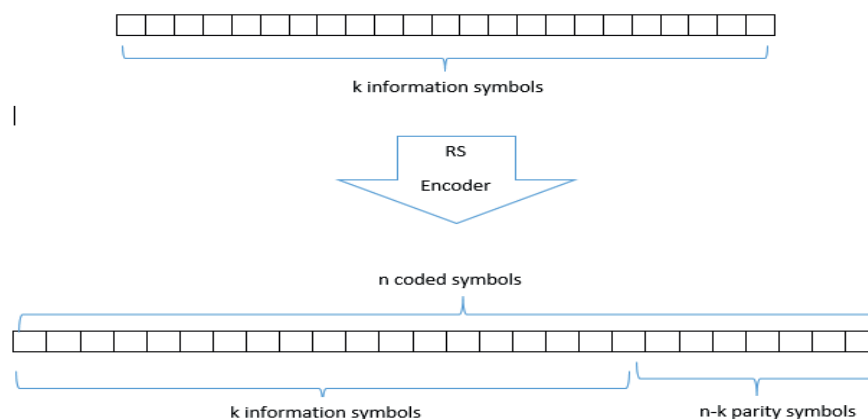


Figure 9: Reed Solomon Code

### 3.9 MAC layer

The MAC protocol is a significant technique that is essential for the effective operation of the network. It controls the access to the communication channel by the sensor nodes that need to transmit data packets. MAC protocols consume energy not only during transmitting or receiving data, but also due to collisions, control packets transmission, overhearing and idle listening. The MAC layer's major function is to determine when a node has access to the shared communication channel and to resolve any potential conflicts between competing nodes. The MAC layer's other responsibility is to correct communication errors that occur at the physical layer and executing other activities such as framing, addressing and flow control [10]. The choice of a MAC protocol has a direct bearing on network transmissions efficiency and reliability due to interference and errors found in wireless communication.

MAC protocols are divided into two categories, contention based and schedule-based protocols. Schedule based protocols are generally based on Time Division Multiple Access (TDMA). This type of protocol is centralised and is appropriate for static network topologies. It employs prior knowledge of the network topology by establishing a schedule by synchronising the clock in every sensor node. This means that slots are allocated for data transfer between the nodes. The contention-based protocol is based on the Carrier Sense Multiple Access (CSMA). With this type of protocol, the sensor nodes compete to access the medium. CSMA has variations, namely collision detection (CSMA/CD) and collision avoidance CSMA/CA). There is another variation where the contention is synchronous or asynchronous. The synchronous scheme uses duty-cycle while the asynchronous scheme uses low power listening.

#### 3.9.1 SensorMAC Protocol

Sensor Medium Access Control (SMAC) is a MAC protocol created to preserve energy and prolong the network lifetime. With this protocol sensor nodes intermittently sleep and wake up; thus, it has two states, the sleep period and the active period as shown in Figure 10. The active period consists of two time periods, SYNC and DATA. The MAC layer contention window size determines the duration of the active interval which is fixed. Depending on the duty-cycle the sleep period could be longer or shorter than the active period. Each node that is part of the network will have identical cycle duration and duty-cycle. SMAC synchronises the sensor nodes by exchanging their sleep-awake schedules contained in the SYNC packets to improve the communication efficiency. Each active phase has a fixed period earmarked for

SYNC packet exchange. To guarantee successful unicast transmissions, SMAC employs RTS/CTS/DATA/ACK packets. Since SMAC comprises a fixed contention window, changing the size of the contention window correspondingly alters the duration of the active period, hence affecting the synchronisation process. On the other hand, when a node successfully transmits an RTS packet, it does not go back to sleep until the transmitted DATA packet is acknowledged.

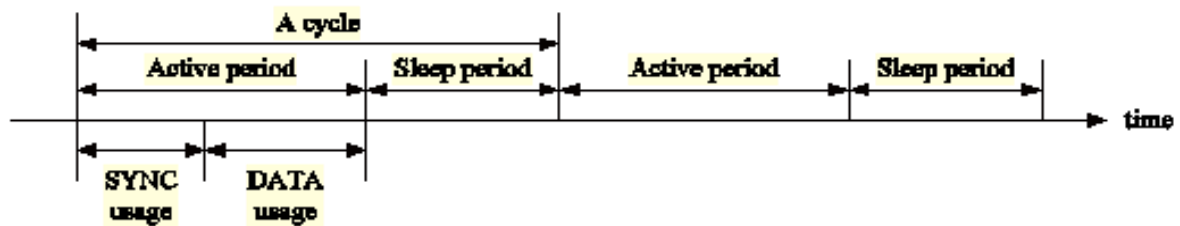


Figure 10: SMAC Sleep-Active Cycle [71]

Before the wake-up/ sleep cycle starts, each sensor node needs to select a work schedule and exchange it with neighbouring nodes. Every sensor node maintains a schedule table to store all the timetables of neighbouring nodes within its vicinity. They use their radios to exchange information on each other's schedules by radio to all existing neighbouring nodes resulting in synchronisation of schedules. The nodes near each other periodically update their timeline in order to prevent the deviation of the cycle listening / sleep time. Updating the schedule is done by exchanging synchronization packets SYNC.

### 3.9.2 Slotted Aloha Protocol

Slotted Aloha is a medium access protocol improved from pure Aloha. Discrete time slots, equivalent to the packet transmission time, were introduced to improve maximum throughput. Packets arrive for transmission according to a Poisson process. Each packet transmitted fits into one of these slots by starting and finishing in exact sync with the slot divisions. If a packet arrives at the sensor node for transmission, it must be deferred until the start of the next slot. If more than one node sends a data packet in the same time slot, the packets collide and none of them are received successfully. The nodes then retransmit the packets until they are successfully transmitted. Figure 11 shows the movement of packets through time slots. The boxes indicate data packets. Packets in the same slot are shown by the shaded boxes which result in collision in that time slot. The shaded slots indicate collisions.

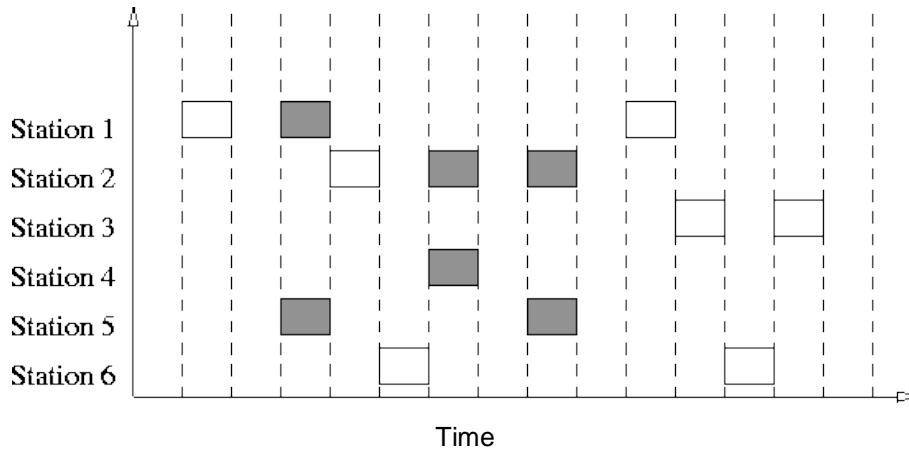


Figure 11: Slotted Aloha Protocol [34]

### 3.10 Network Traffic

In wireless sensor networks, a mathematical approximation for real traffic behaviour is used and known as a traffic model. Generally, there can be more than one potential model for the same traffic source, but the selection is application dependent. The selection of the traffic model often depends on the performance requirements, whether simple and less accurate, or accurate and more complex. A traffic model that is ideal would be both simple and accurate, but typically, there is trade-off between accuracy and simplicity. Initial network models were based on telephony networks. One of the most widely used and oldest traffic models is the Poisson Model. This memoryless distribution is the prime model used for analysing traffic. Traffic models have three major uses. One important use is to properly scope network resources for a target level of QoS. Another vital use is the verification of network performance under explicit traffic scenarios.

### 3.11 Markov chains

Markov chains are a type of stochastic process that moves from one state to the next. In this process, a finite number of elements is denoted with real positive numbers, defined by a set as  $\{S_t, t = 0, 1, 2, \dots, n\}$  with a finite number of elements and denoted with real positive numbers.  $S_t = i$  denotes that the process is state  $i$  at a time instant  $t$  and assume discrete values [72]. The Markov chain moves from state  $i$  to state  $j$  in the next time  $t$  at a fixed probability  $p_{ij}$  as shown in Equation (3). A stochastic process is said to have the Markov property if successive states of the random variable depend only on its current state. Consequently, a future state or value of a variable depends solely on its preceding state, with no dependence on the states before

that. This means that the state in which the system finds itself at time step  $n + 1$  is depended on where it is at time step  $n$ .

$$P\{S_{n+1} = s_{n+1} | S_n = s_n, \dots, s_1\} = P\{S_{n+1} = s_{n+1} | S_n = s_n\}. \quad (3)$$

Therefore, the conditional probability of making a transition from state  $s_n = i$  to  $s_{n+1} = j$  is given by

$$p_{ij}(n) = P\{S_{n+1} = j | S_n = i\}. \quad (4)$$

where,

$S_n$  is the current system,

$S_{n+1}$  is the future system,

$s_n$  is the state of the system at time step  $n$ .

A transition probability matrix is formed by placing  $p_{ij}(n)$  in row  $i$  and column  $j$  as shown in Equation (5).

$$P = \begin{bmatrix} p_{00}(n) & p_{01}(n) & p_{02}(n) & \dots & p_{0j}(n) \\ p_{10}(n) & p_{11}(n) & p_{12}(n) & \dots & p_{1j}(n) \\ p_{20}(n) & p_{21}(n) & p_{22}(n) & \dots & p_{2j}(n) \\ \vdots & \vdots & \vdots & \ddots & \vdots \\ p_{i0}(n) & p_{i1}(n) & p_{i2}(n) & \dots & p_{ij}(n) \end{bmatrix}. \quad (5)$$

The elements of the matrix  $P(n)$  fulfil the following properties:

$$0 \leq p_{ij}(n) \leq 1. \quad (6)$$

And for all  $i$

$$\sum_{all j} p_{ij}(n) = 1. \quad (7)$$

Markov chains have three important elements, namely transition diagram, transition matrix and steady state vector. Each element in the probability transition matrix  $\mathbf{P}$  signifies the probability that the system shifts or remains in its current state. These shifts are known as transitions. The probability transition matrix can be characterised as a diagram known as the transition diagram. Every node in the transition diagram denotes a state of the Markov chain specified by a number. Arrows connect state  $i$  to state  $j$  if a transition exists and the transition probability  $p_{ij}(n)$  is written on the linking arrows. The transition diagram is an easy way to see the possible shifts between states according to the probability as shown in Figure 12.

In a Markov chain, an absorbing state is a state where once it is reached it is impossible to leave. This happens when all the sensor nodes have managed to transmit a data packet. The

property of an absorbing Markov chain is that as the powers of the transition matrix approach a limiting matrix, the steady-state vector  $\pi$ , expresses the long-term probability of ending up in any of the states, regardless of which state you started in. It is the probability that one of the states will approach a limiting value as time goes to infinity. On the other hand, in the distant future, there would be very little change in the probabilities from one transition to the next. These limiting values are known as ‘stable probabilities’. If the system is started off so that each state has probability equal to its stable probability, then these probabilities recur infinitely resulting in the system being in a ‘steady state’.

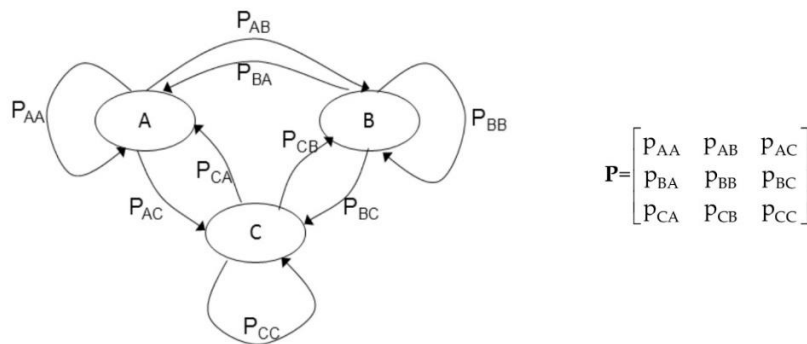


Figure 12: Probability transition diagram for a 3-state Markov chain

When an absorbing transition matrix is decomposed, it is arranged in a standard form into an identity matrix I, a zero matrix O, a non-zero matrix R and a non-absorbing state matrix Q. A fundamental matrix F is derived from the decomposed transition matrix, where we have  $F = (I - Q)^{-1}$ . The fundamental matrix is a very important feature as its entries provide the required number of steps that the process is at node  $j$  if it started on node  $i$ . The total number of expected steps before absorption can be found by adding the number of entries in the relevant row of node  $i$  in the fundamental matrix. When we multiply the fundamental matrix by the matrix R, it gives the probability that if we start at node I we end up in the absorbing state at node  $j$ .

### 3.12 Chapter Conclusion

In this chapter, the components of the wireless sensor network were broken down and their functions in the communication system discussed. The operation of the physical layer and medium access control layers SMAC and SALOHA were decrypted. The role of error control coding in the PHY layer and the Markov chain process for the MAC layer were outlined. The network traffic model employed in the Markov process was presented. The next chapter discusses the design of the proposed solution.

## CHAPTER FOUR: DESIGN OF THE PROPOSED SOLUTION

### 4.1 Introduction

Wireless sensor networks waste energy through idle listening, overhearing, interference and collision. This requires the utilisation of effective strategies to minimise energy consumption and hence extend network life. The purpose of this study is to investigate an energy consumption model by jointly tuning the PHY and MAC layers of a Wireless Temperature Sensor Network to design and implement a mechanism that will provide or result in energy savings in WTSNs. Thus, the proposed solution is to design and implement a mechanism that will conserve energy in WTSNs. To investigate the energy consumption model of the WTSN that improves communication performance, the approach uses a Markov chain model, analytic derivations and simulations through 802.11g with AWGN signals. The model framework in [49] is used for cross-layer optimisation in this research. The research employs a star topology network to study the energy efficiency of varied RS code rates including a case without coding using SensorMAC (SMAC) and Slotted Aloha (S-Aloha) as medium access protocols. The research evaluates the mean number of steps required by the sensor nodes to successfully send a data packet during the transmission phase using a Markov chain model.

### 4.2 Research Design

A simulation and statistical modelling approach was used in the research. The model was simulated in MATLAB and an analysis of the probability of successful channel access, successful packet transmission and new packet arrivals was conducted. It facilitated the determination of the number of steps required for every sensor node to have reported its observation to the sink node successfully. When the length of each step was known, the sum of steps to absorption could then be converted into time to absorption. Knowledge of the time to absorption enabled the analysis of the impact of tuning the parameters of the protocol stack. Varying these variables influenced the amount of energy consumed for all the sensors to transmit to the sink node. The baseline case was the physical layer without any error coding. The following assumptions were used in the research:

- (a) The sensor nodes are homogenous.
- (b) The sensor nodes are stationary, and their position will not change after deployment.
- (c) The sink node is a full function device and receives all the traffic from the sensor nodes
- (d) A sensor node does not generate a new packet for transmission until the previous one is delivered successfully.

### 4.3 Network Setup

The wireless temperature sensor network is a star topology that comprised twenty homogenous sensor nodes that are stationary and whose position would not change after deployment. The sink node is a full function device and received all the data streams from the sensor nodes and could communicate with other sink nodes within the specified range. The sensor nodes did not generate new packets for transmission pending the successful delivery of the previous packet. The activities of this network setup took place as follows:

- (i) Sensor node detects a spike in the temperature reading.
- (ii) Sensor node sends a wake-up signal to the sink node.
- (iii) Sink node decodes the wake-up signal successfully and is awakened.
- (iv) Sink node turns on the data radio.
- (v) A beacon message is sent to the sensor nodes for synchronisation with the sink node and to identify when they will attempt to access the channel
- (vi) Beacon message contains information about the length of the transmission slot and its starting time.
- (vii) There are  $M$  nodes with a data packet to transmit.
- (viii) If  $M-1$  nodes independently sense a spike in temperature after the first node transmission period has started, it is assumed that for these nodes, either their timer has not expired or the spike in the temperature reading is not critical enough to trigger the transmission of the wake-up signal to the sink node.
- (ix) Every sensor node transmits in a slot determined by the sink node. Once sensor nodes receive the beacon message, they are then able to transmit the data packets during the allocated transmission slot.
- (x) Sink node allocates reserved time slots to every node that needs to communicate with the sink node by sending the acknowledge message (ACK).
- (xi) If there is a single transmission in a slot, there will be no collision and the probability of success hinges on the bit error probability at the receiver detection process.
- (xii) If the transmission is unsuccessful owing to collisions or channel errors, the nodes attempt to retransmit the packet in a new slot.
- (xiii) If the transmission is successful, the node will enter a sleep mode.
- (xiv) Throughout the transmission period, new packets can arrive independently at each node with a certain probability. The nodes do not support buffering of data packets, but a new packet can replace the old packet, in which case the node transmits only the latest sensor observation.

- (xv) The transmission period ends when each node has successfully sent its data packet and entered a sleep mode.
- (xvi) The number of nodes that do not have a packet to transmit at the beginning of the competition period cannot be larger than  $M$  during the transmission period because it is assumed that the nodes that do not have a packet to transmit at the beginning of the competition period will stay in sleep mode and transmit their observations on the next transmission period.

#### 4.4 Transmission Period

The network nodes employed the wake-up signal at the commencement of the period of transmission. The study focused on:

- (i) The period of transmission that followed a wake-up signal.
- (ii) The resulting energy consumption experienced due to channel competition
- (iii) The number of transmissions for the completion of a successful communication.

Sensor node A detects a spike in temperature and sends a wake-up signal. The sink node successfully decodes the wake-up call and switches on the data radio. A beacon message would be transmitted using the data radio or if a specific timer has expired after the preceding transmission period. For the sake of simplicity, propagation delay was neglected. The beacon message would contain information about the length of the transmission period slot, and the starting time. Let  $M$  be the number of nodes that have a packet of data to transmit. Assuming  $M-1$  other sensor nodes also sensed the change in temperature after the preceding transmission period, it was assumed that the temperature change was not critical enough, or that their timer had not expired to be able to generate the wake-up signal transmission to the sink node. After the  $M$  sensor nodes received the beacon message, they would then be able to send their data packets during the transmission period. If a collision occurred, the nodes would have to retransmit their data packets. To curb that problem of collision, the sink node would allocate reserved time slots for each sensor node that required communication with the sink node.

An assumption of a positive acknowledgement (ACK) scheme for the MAC layer was adopted. The sink node would send an ACK message after receiving a packet successfully. If the sensor node failed to receive the ACK message, it would resend the packet until it is successfully received by the sink. Failed transmission may be the result of errors caused by fluctuations in the wireless channel or due to collisions occurring during the channel access competition. New

packets could independently arrive at each of the M nodes during the transmission period. The assumption was that a sensor node would not generate a new packet for transmission until the previous one was delivered successfully. This meant that the nodes did not support buffering. Additionally, the number of nodes with a packet to transmit, could not become larger than M during the transmission period because it was assumed that the nodes that did not have a packet to transmit at the beginning of a competition period would stay in sleep mode and transmit their observations on the next transmission period.

This research used a mathematical model to analyse the transmission period in the WTSN setting. A Markov chain model was employed to estimate the length of the transmission period taking into consideration the PHY and MAC layer parameters. The objective of the Markov chain was to study the number of steps needed such that each node reported its observation to the sink node successfully. The number of steps to absorption could then be converted into time to absorption when the length of each step was identified. Knowing the time to absorption allowed for the evaluation of the effect of tuning the protocol stack parameters. In this case, tuning the transmission power, the method of modulation and channel access and error correction coding rate aimed to reduce the number of retransmissions and thus shortening the length of the transmission period.

#### 4.5 Physical Layer Tuning

Binary modulation was employed to allow the communication system to send data at the least power expenditure that is practicable. Energy consumption for uncoded and coded transmission was determined by computing the bit error probability during transmission. Calculating the packet transmission probability provided one of the inputs of the Markov chain model to calculate the state transition probabilities. Table 1 shows the characteristics of the transceivers used in the study.

Table 1: Physical Layer Characteristics for the Transceivers

Characteristic	802.11g
Frequency Band	2.4GHz
Modulation	BPSK
Spreading Method	OFDM
Communication Range	40m
Bandwidth	20MHz
Transmission Scheme	CSMA/CA
Channel	AWGN

The BER performance of the uncoded OFDM system over the AWGN channel is given by:

$$P_b = Q \left[ \sqrt{\frac{2E_b}{N_0}} \right] = \frac{1}{2} \operatorname{erfc} \left( \sqrt{\frac{E_b}{N_0}} \right). \quad (8)$$

where  $P_b$  is the bit error probability with “b” bits per symbol.

The packet error probability (PEP) will thus be given by:

$$PEP = 1 - (1 - P_b)^D. \quad (9)$$

where D is the length of the packet in bits = 127bytes = 1016bits.

The desired BER:  $P_b = 10^{-5}$

The BER performance of the Reed Solomon coded OFDM system over the AWGN channel is given by:

$$P_{b,i} = Q \left( \frac{2E}{N_0} \right). \quad (10)$$

Where  $E = r_i E_b$  and  $r_i$  is the  $i^{\text{th}}$  code rate

The project explores the possible energy gains that could be accomplished by tuning the rate for forward error correction, in this case Reed-Solomon Codes.

RS code operates with the following parameters:

- (a) Symbol length: bits per symbol  $b = 6$ .
- (b) Block length:  $n = 2^b - 1$ , symbols.
- (c) Message data length:  $k = 2^b - 1 - 2t$ , symbols.
- (d) Redundant/parity bits:  $t = \{3, 4, 5, 6, 7, 8\}$
- (e) Size of parity check code:  $n - k = 2t$  symbols.
- (f) Code rate:  $r = k/n$ .

Other code rates were exploited to study performance of the network in terms of energy utilisation. SMAC and S-Aloha protocols were used as media access control and a comparison done between the two protocols, that is for  $t = \{3, 4, 5, 6, 7, 8\}$ .

Symbol error probability before decoding

$$P_{sym,i} = 1 - (1 - P_{b,i})^b. \quad (11)$$

Decoded symbol error probability in the case of hard decision

$$P_{ds,i} = \frac{1}{n} \sum_{e=t+1}^n \binom{n}{e} P_{sym,i}^e (1 - P_{sym,i})^{n-e}. \quad (12)$$

The packet error probability ( $PEP_i$ ) will thus be given by:

$$PEP_i = 1 - (1 - P_{ds,i})^{X_i}. \quad (13)$$

Where  $X_i = \frac{D_i}{b}$  and is the number of code symbols in a packet,

$D_i = \frac{D}{r_i}$  is the packet length when using code rate  $r_i$ .

#### 4.6 MAC Layer Tuning

The nodes that require to communicate with the sink node are not known at any given time because that hinges on the number of nodes that have data packets to transmit. The MAC layer is optimal when there is maximum channel access for the transmission of a packet to take place. Finding the probability of successful channel access provided input to compute the state transition probabilities in the Markov chain model. The probability that any node has accessed the channel in a slot is given by:

$$P_{succ}^{MAC}(p) = Mp(1-p)^{M-1}. \quad (14)$$

The probability that  $j$  nodes successfully accessed the channel is given by:

$$P_{succ}^{MAC}(p) = (M-j)p(1-p)^{M-j-1}. \quad (15)$$

where  $M$  is the number of nodes competing for channel access in a slot with probability  $p$

By computing the derivative of Equation (14), the maximum channel access efficiency can be established at the value of zero:

$$P_{succ}^{MAC} = (p^*)' = 0, \quad (16)$$

which occurs when  $p^* = \frac{1}{M}$ , explicitly, when the quantity of slots in the transmission period matches the number of nodes competing for the channel. This scenario corresponds to the traffic load  $G = 1$ ,

where  $G$  is the offered traffic load.

Therefore, the maximum channel access success probability can be calculated as

$$P_{succ}^{MAC}(p^*) = (1 - 1/M)^{M-1}. \quad (17)$$

The values of  $p$  used in the project are:  $p = \{0.05, 0.1, 0.2, 1/(M-j)\}$ .

#### 4.7 Network Traffic Generation

In this event-driven wireless temperature sensor network, the traffic arrival process was modelled using the Poisson process. The network traffic load is expressed as

$$G = \theta T_f, \quad (18)$$

where  $\theta$  is the average packet arrival rate per second and

$T_f$  is the duration of uncoded data transmission.

If the data transmission is coded, the packet duration is affected by the coding overhead, by the component  $1/r_i$  and as such, the slot interval needs to accommodate this overhead. In this project, it was assumed that  $a = \zeta$  new packets arrive independently at each node during a time period  $\tau$  according to a Poisson probability distribution with  $\rho$  packets / s.

$$P_r(a = \zeta) = \frac{(\rho\tau)^\zeta}{\zeta!} e^{-\rho\tau}. \quad (19)$$

where  $\tau$  is the time period for the Poisson process and

$\rho$  is the arrival rate for the Poisson process

$P_\Omega(\Omega=k)$  is defined to be the probability that  $\kappa = 0, 1, \dots, j$  node(s) will have a new packet to transmit according to a Poisson probability distribution. Table 2 shows the values used to generate the network traffic.

Table 2: Values for Generating Network Traffic

$\rho$	0.05 pkt/s
$\tau$	20s
$\zeta$	10
$\rho\tau$	1

#### 4.8 Markov Chain Model

There are events that can transpire in the Markov chain model including the following:

- (i) Successful channel access & successful transmission & no new arrivals => move from state  $j$  to state  $j + 1$ ; Probability for event 1 is defined as:

$$P_{(1)} = P_{succ}^{MAC} P_{succ}^{PHY} P_\Omega(\Omega = 0). \quad (20)$$

- (ii) Successful channel access and successful transmission and  $\kappa$  node(s) have a new packet=> move from state  $j$  to state  $j - \kappa + 1$ ; Probability for event 2 is defined as:

$$P_{(2)} = P_{succ}^{MAC} P_{succ}^{PHY} P_\Omega(\Omega = \kappa). \quad (21)$$

- (iii) Unsuccessful channel access and no new arrivals => stay in state  $j$ ; Probability for event 3 is defined as:

$$P_{(3)} = P_{fail}^{MAC} P_\Omega(\Omega = 0). \quad (22)$$

(iv) Successful channel access and unsuccessful transmission and no new arrivals => stay in state  $j$ ; Probability for event 4 is defined as:

$$P_{(4)} = P_{succ}^{MAC} P_{fail}^{PHY} P_{\Omega} = (\Omega = 0). \quad (23)$$

(v) Unsuccessful channel access and  $\kappa$  node(s) have a new packet => move from state  $j$  to state  $j - \kappa$ ; Probability for event 5 is defined as:

$$P_{(5)} = P_{fail}^{MAC} P_{\Omega} (\Omega = \kappa). \quad (24)$$

(vi) Successful channel access and unsuccessful transmission and  $\kappa$  node(s) have a new packet => move from state  $j$  to state  $j - \kappa$ ; Probability for event 6 is defined as:

$$P_{(6)} = P_{succ}^{MAC} P_{fail}^{PHY} P_{\Omega} (\Omega = \kappa). \quad (25)$$

To calculate the probabilities for the state transitions for the distinct events in the Markov chain model, knowing the following probabilities is imperative.

- (i) The probability of successful channel access ( $P_{succ}^{MAC}$ ),
- (ii) The probability of successful packet transmission ( $P_{succ}^{PHY}$ ),
- (iii) The probability of new packet arrivals ( $P_{\Omega} (\Omega = \kappa)$ ).

For the scenario when one sensor node has successful channel access, successful transmission and no new arrivals happening at that node, the probability of state transition is:

$$P_{0,1} = P_r \{S_{t+1} = 1 | S_t = 0\} = Mp(1-p)^{M-1} P_q P_{succ}^{PHY}, \quad (26)$$

where  $S_t$  and  $S_{t+1}$  represent the value of the state at the event times  $t$  and  $t + 1$ , respectively.

$M$  is the number of nodes competing for the channel access at the state  $S_t$ .

$P_{0,1}$  is the probability for moving from state 0 to 1.

The probability of success in the PHY layer,  $P_{succ}^{PHY} = 1 - PEP$ , may be computed by applying Equation (9) and Equation (13) for the scenario with no coding and the coded scenario respectively.

The probability that no new packet arrives at the node's queue is given by

$$P_q = P_r(a = 0) = 1 - P_a, \quad (27)$$

where  $P_a = P_r(a > 0)$  is the probability that new packets arrive at the node's queue.

The probability of remaining in the starting state is:

$$P_{0,0} = P_r \{S_{t+1} = 0 | S_t = 0\} = 1 - P_{0,1} = 1 - Mp(1-p)^{M-1} P_q P_{succ}^{PHY}, \quad (28)$$

which means none of the sensor nodes successfully transmit a packet and the system stays in its starting state. The probability of that event is the complement of the probability that any of the  $M$  nodes is successful.

The probability of transition from state  $j$  to state  $j + 1$  is defined as:

$$P_{j,j+1} = P_r\{S_{t+1} = j + 1 | S_t = j\} = (M - j)p(1 - p)^{M-j-1}[P_q]^{j+1}P_{succ}^{PHY}. \quad (29)$$

In this instance, one of the  $(M - j)$  nodes that have a packet to transmit, successfully access the channel and transmits the packet successfully with no new packets arriving at the nodes that do not have anything to transmit in their queue. The probability of transition of remaining in state  $j$  should also be computed putting into consideration the situation where new packet arrivals occur. In that circumstance, the Markov chain shifts  $\kappa$  steps towards the starting state. In the case that the system is in state  $j$  and one node successfully transmits a packet, it implies that at most  $\kappa = j + 1$  sensor nodes can have a new packet arrival. However, in the case where packet transmission is not successful while the chain is in the starting state  $j$ , it means at most  $\kappa = j$  nodes can have a new packet arrival. Consequently, the probability of the chain transitioning  $\kappa$  steps towards its starting state is given as:

$$\begin{aligned} P_{j,j-\kappa} &= P_r\{S_{t+1} = j - \kappa | S_t = j\} \\ &= (M - j)p(1 - p)^{(M-j-1)} \binom{j+1}{\kappa+1} [P_a]^{\kappa+1} [P_q]^{j-\kappa+1} P_{succ}^{PHY} \\ &\quad + (1 - (M - j)p(1 - p)^{M-j-1}) P_{succ}^{PHY} \binom{j}{\kappa} [P_a]^\kappa [P_q]^{j-\kappa}, \end{aligned} \quad (30)$$

where  $\kappa = [1, \dots, j]$ . For the case  $\kappa = 0$ , the probability  $p_{j,j}$  for remaining in the same state is calculated using Equation (30). By utilising the probabilities of state transition for the Markov chain, the number of steps required to move from state 0 to state  $M$  can be evaluated, where every sensor node has transmitted its packet(s) successfully as explained in the next section.

#### 4.9 Time to Absorption

Decomposing the matrix  $\mathbf{P}$  gives:

$$\mathbf{P} = \begin{bmatrix} \mathbf{V} & \mathbf{R} \\ \mathbf{0}^T & \mathbf{1} \end{bmatrix}, \quad (31)$$

where the matrix  $\mathbf{V}$  consists of elements  $V_{x,y} = P_{x,y}$  for  $x, y = 0, 1, \dots, M - 1$  and  $\mathbf{R}^T = [0 \ 0 \ \dots \ P_{(M-1),M}]$ .

The fundamental matrix for the absorbing chain is defined as:

$$\mathbf{A} = [\mathbf{I} - \mathbf{V}]^{-1}, \quad (32)$$

which is composed of elements  $\lambda_{x,y}$  for  $x, y = 0, 1, \dots, M - 1$ . If the initial state is

$S = 0$ , then the mean number of steps to absorption is:

$$\Gamma_0 = \sum_y \lambda_{0,y}. \quad (33)$$

The duration of single step (slot) must be such that the data packet can be transmitted and the following ACK message can be received successfully, that is, the slot duration given as:

$$T_{slot,i} = T_{f,i} + T_{MaxAckWait} + T_{ACK}, \quad (34)$$

where  $T_{f,i} = T_f/r_i$  (and for the uncoded case  $r_i = 1$ ) is the interval of a data frame (payload and headers included) comprising the redundancy caused by the code rate  $i$ .

$T_{MaxAckWait}$  is the maximum time a node waits for an ACK frame before retransmitting a data packet.

$T_{ACK}$  is the duration of an ACK frame.

Therefore, the expected time to absorption when using code rate  $i$  can be calculated as

$$\Theta_i = \Gamma_0 T_{slot,i}. \quad (35)$$

#### 4.10 Transmission Period Analysis

A MATLAB simulation was used to detect the number of collisions, total number of transmitted packets and the number of idle slots spent during the transmission period. The values of bit error probability calculated analytically were utilised in the simulation model for the evaluation of the probability of successful transmission in the physical layer. A comparison of the analytical results and the simulation results was done in two ways to validate the correctness of the models:

- (i) Results from the Markov chain model should match the simulation model results regarding the number of steps to absorption; and
- (ii) For a boundary scenario case, where there are no new packet arrivals during the competition period, the simulation results about the expected number of required transmissions to reach absorption should also match the analytical results.

The analytical derivation of the required number of transmissions needed to reach absorption was done as described below. The mean number of steps required to transmit successfully when at Markov chain state  $j$  was obtained using Equation (29) The average number of steps needed for a node to be successful when at Markov chain state  $j$ , was derived using Equation (29), without considering the probability of new packet arrivals, as follows:

$$N_{steps,j} = \frac{1}{(M-j)p(1-p)^{(M-j-1)}P_{succ}^{PHY}}. \quad (36)$$

The expected number of transmissions that occur during a step, at state  $j$ , is computed as follows:

$$E\{X_j\} = \sum_x P[X = x]x. \quad (37)$$

where  $x = [1, \dots, M - j]$  and the probability that  $x$  nodes attempt to transmit at state  $j$  can be calculated as [16]

$$P_r[X = x] = \frac{G_j^x e^{-G_j}}{x!}. \quad (38)$$

where  $G_j = p(M - j)$  is the offered traffic load at state  $j$ . The average number of transmissions required to arrive at the absorption state could therefore be calculated by taking into account all the states of the Markov chain as stated below:

$$N_{tx,MC} = \sum_{j=0}^M N_{steps,j} E\{X_j\}. \quad (39)$$

The average number of transmissions could be computed analytically using Equation (39) and compared with corresponding results from the simulation.

#### 4.11 Energy Consumption

The model for energy consumption that was employed for the evaluation of the impact of 802.11 PHY layer, SMAC and S-Aloha MAC layers on the energy utilisation of the star topology network under study is described in this section. The model that was proposed could be used to compute the amount of energy depleted from the start of the period of transmission until each node has transmitted its packet(s) successfully. To compute energy consumption of the network, there is a need to know the power consumption for transmission and reception at the PHY and MAC layers. At the PHY layer, the power dissipated and hence the corresponding energy cost of a transmission has two components; the internal circuitry consumption and the radio frequency consumption (RF) which is expressed as:

$$P_{tx,i} = r_i P_{tx,RF} + P_{tx,circ}. \quad (40)$$

where the RF element is attributed to proportion of the energy content of the data packet with the applied code rate, meaning,  $P_{tx,RF}$  would be multiplied by the applicable code rate  $r_i$ . This is because the energy per coded bit depends on the code that is being applied, as explained in Section 4.5.

The power consumption of the receiver,  $P_{rx}$ , is attributed to the power consumed by every element at the receiver. The consumption of energy at the PHY layer for the transmission and reception of a packet could then be computed for code rate  $i$  as shown below:

$$E_{tx,i}^{PHY} = (r_i P_{tx,RF} + P_{tx,circ}) T_{f,i}. \quad (41)$$

$$E_{rx,i}^{PHY} = P_{rx} T_{f,i}. \quad (42)$$

The factors that affect energy consumption in the MAC layer are calculated in the following manner:

$$E_{tx,f}^{MAC} = P_{rx} T_{MaxAckWait},$$

$$E_{tx,s}^{MAC} = P_{rx} T_{MaxAckWait} + P_{rx} T_{ACK},$$

$$E_{rx}^{MAC} = P_{tx} T_{ACK},$$

$$E_{Imp}^{MAC} = P_{idle} T_{idle},$$

where  $T_{idle}$  is the length of the idle slot and  $P_{idle}$  is the power consumption in the idle mode.

Using the energy consumption model given as:

$$E_{TP} = n_{tx}^{fail} (E_{tx}^{PHY} + E_{tx,f}^{MAC}) + n_{tx}^{succ} (E_{tx}^{PHY} + E_{tx,s}^{MAC} + E_{rx}^{PHY} + E_{rx}^{MAC}) + E_{Imp}^{MAC} \quad (43)$$

and the derivations above, the computation of the network's average energy consumption when applying  $i^{\text{th}}$  code rate may be accomplished as follows:

$$E_{TP,i} = n_{tx}^{fail} (P_{tx,i} T_{f,i} + P_{rx} T_{MaxAckWait}) + n_{tx}^{succ} (P_{tx,i} T_{f,i} + P_{rx} T_{MaxAckWait} + P_{rx} T_{ACK} + P_{rx} T_{f,i} + P_{tx} T_{ACK}) + n_{idle} P_{idle} T_{idle}. \quad (44)$$

where  $n_{tx}^{fail}$  is the number of failed transmissions (due to MAC layer collision or PHY transmission errors) for the whole network,

$n_{tx}^{succ}$  is the successful number of transmissions,

$n_{idle}$  is the total number of idle slots spent throughout the transmission period.

The parameters  $n_{tx}^{fail}$ ,  $n_{tx}^{succ}$  and  $n_{idle}$  were obtained from the MATLAB simulations. For the case where no new packet arrivals occur, the analytical derivations presented earlier could be used to determine the average number of  $n_{tx}^{fail}$  and  $n_{tx}^{succ}$ .

$E_{tx}^{PHY}$  is the PHY layer factor on the energy consumption of a Tx-node,

$E_{tx,f}^{MAC}$  is the effect of the MAC protocol on the energy consumption of a Tx-node in the case when transmission fails.

$E_{tx.s}^{MAC}$  is the effect of the MAC protocol on the consumption of energy at the Tx-node when transmission is successful.

$E_{rx}^{PHY}$  and  $E_{rx}^{MAC}$  are the energy consuming factors of the PHY and MAC layers at the receiving node respectively.

The MAC protocol contains imperfections which cause energy consumption during transmission. A factor called  $E_{imp}^{MAC}$  is included in the calculations to cater for these imperfections whose value is depended on the MAC layer features. For instance, the parameter could represent the consequence of a back-off strategy resulting in idle slots, which are existent in the transmission periods. In an ideal SMAC, there would be no idle slots throughout the period of transmission and, consequently,  $E_{imp}^{MAC}$  would be a zero. For MAC protocols that are competition-free,  $E_{imp}^{MAC}$  could be attributed to the energy consumption overhead triggered by the scheduling of slots and for synchronisation.

#### 4.12 Design Specifications for Implementation

The specifications for the WTSN design are given in Table 3.

Table 3: Parameter Values Employed for Performance Evaluation

Parameter	Definition	Value
b	Bits per coded symbol	6
N	Number of nodes in the network	20
M	Number of nodes with packet to transmit at the initial state	20
P	Probability to transmit in a slot	0.05,0.1,0.2, 1/(M-j)
$\rho$	Arrival rate for Poisson arrival process	0.05events/sec
$L_{PMH}$	Payload and MAC layer header	130 bytes
$L_{PH}$	PHY layer header	6 bytes
$L_{ACK}$	ACK frame size	14 bytes
$L_{CTS}$	CTS frame size	14 bytes
$L_{RTS}$	RTS frame size	20 bytes
$L_{PRE}$	Preamble length	18 bytes
SIFS	Short inter-frame space	10 $\mu$ s
DIFS	Distributed Coordination Function inter-frame space	28 $\mu$ s
CW	Contention Window size	0-15
$T_{MaxWaitACK}$	Maximum wait time for ACK frame	160 $\mu$ s
R	Bitrate in Mbps	1Mbps
$P_{tx,circ}$	Transmitter circuitry power consumption	60mW
$P_{tx,RF}$	Transmitter RF power component	6mW
$P_{idle}$	Idle mode power consumption	2mW
$P_{rx}$	Receiver power consumption	40 $\mu$ W

#### 4.13 Chapter Conclusion

In this chapter the design of proposed solution to conserve energy was outlined. The layout explained the determination of the transmission period and how it relates to time to absorption. The tuning of the PHY layer with and without encoding was explained in detail. The MAC layer tuning involving different channel access probabilities and the generation of the network

traffic using the Poisson process was expounded. A description of the transition states of the Markov chain was given, laying out how the transition state probabilities are determined. The details of how the energy consumption is determined were given and a list of the design specifications was provided. The next chapter provides the implementation details.

## CHAPTER FIVE: IMPLEMENTATION

### 5.1 Introduction

This chapter presents the implementation of the prototype. The description of the simulation tools that were employed is detailed. Among numerous simulation platforms for simulating wireless sensor networks, MATLAB is the simulation environment suitable for this research. The power of this simulation technique lies in its ability to accommodate the changes to different PHY layer parameters which aids in studying their effect on network behaviour. Building the sensor nodes and sink nodes is straightforward. MATLAB provides a variety of modulation and encoding and communication channel modelling plus various methods to monitor and record the results using the rich library of MATLAB/Simulink [66]. “The name MATLAB stands for matrix laboratory. MATLAB, developed by MathWorks Inc., is a software package for high performance numerical computation and visualisation. The combination of analysis capabilities, flexibility, reliability, and powerful graphics makes MATLAB the premier software package for scientific researchers. MATLAB provides an interactive environment with hundreds of reliable and accurate built-in mathematical functions. These functions provide solutions to a broad range of mathematical problems. MATLAB features a family of application-specific solutions called toolboxes which allow you to learn and apply specialised technology. Toolboxes are comprehensive collections of MATLAB functions (M-files) that extend the MATLAB environment to solve particular classes of problems. The most important feature of MATLAB is its programming capability, which is very easy to learn and to use, and which allows user-developed functions. It also allows access to Fortran algorithms and C codes by means of external interfaces. There are several optional toolboxes written for special applications such as signal processing, control systems design, system identification, statistics, neural networks, fuzzy logic, symbolic computations, and others. MATLAB has been enhanced by the very powerful Simulink program”.

Simulink is a software package for modeling, simulating, and analyzing dynamical systems. It supports linear and nonlinear systems, modeled in continuous time, sampled time, or a hybrid of the two. Systems can also be multi-rate, i.e., have different parts that are sampled or updated at different rates. For modeling, Simulink provides a Graphical User Interface (GUI) for building models as block diagrams, using click-and-drag mouse operations. Simulink includes a comprehensive block library of sinks, sources, linear and nonlinear components, and connectors. With Simulink one is able to create and customise their own blocks. The models

are hierarchical in nature, providing intuition on the organisation of the model and the interaction of its components. After defining the model, simulation is done using a selection of incorporation methods from Simulink menus or by entering commands in MATLAB's command window. Convenient for interactive work, while the command-line approach is very useful for running a batch of simulations (for example, if you are doing Monte Carlo simulations or want to sweep a parameter across a range of values). Using scopes and other display blocks, the simulation results can be seen while the simulation is running. In addition, parameters can be changed and the effect can be seen instantly, for "what if" exploration. The simulation results can be put in the MATLAB workspace for post processing and visualization. Because MATLAB and Simulink are integrated, the models can be simulated, analysed, and revised in either environment at any point [68].

## 5.2 Simulation Environment

In this research the main toolboxes that are applicable are WLAN System Toolbox and Communication System Toolbox and SimEvents. "WLAN System Toolbox provides standard-compliant functions for the design, simulation, analysis, and testing of wireless LAN communications systems. The system toolbox provides configurable physical layer waveforms for IEEE 802.11g standard. It also provides transmitter, channel modelling, and receiver operations, including channel coding, modulation." [69] The Communication System Toolbox is used to design and simulate the physical layer model of the wireless sensor network. It provides the algorithms including channel coding, modulation and OFDM which enable the composition of the physical layer model for the WTSN. SimEvents offers a simulation engine for discrete-events and a library of components for the analysis of event-driven system models and optimising performance characteristics such as packet loss and latency. There are numerous predefined blocks that are available in SimEvents, such as servers and queues, that enable modelling and prioritisation of scheduling and communication. The simulation is used to establish the transmission of information over a communication channel and analysing the performance in the presence of noise and parameter tuning. Figure 13 shows the setup in the simulation environment.

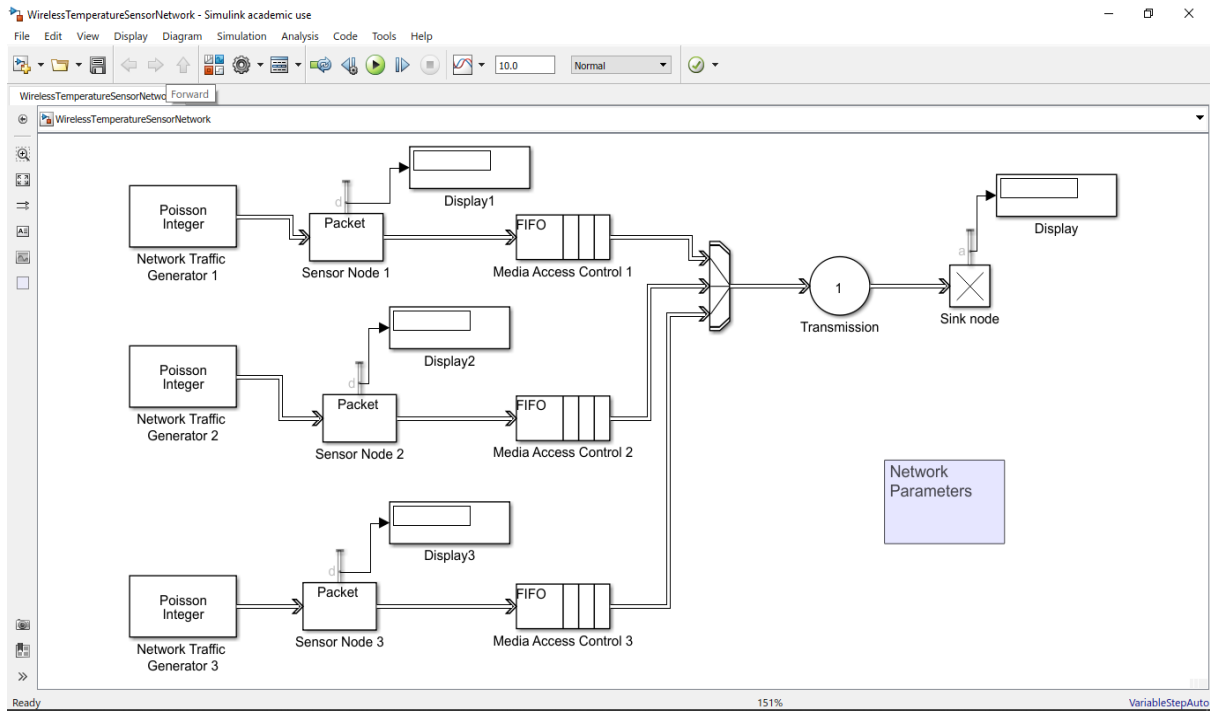


Figure 13: Simulation Environment Setup

The network consists of twenty sensor nodes (sources) that send samples of data they measure to a sink node. The MATLAB Simulink communication block set is used to build a complete transceiver system of the WSN. The WLAN System Toolbox functionality enables the modelling of IEEE 802.11 standardised implementations of the physical layer. It focuses on the Physical Medium Dependent (PMD) and the Physical Layer Convergence Procedure (PLCP) sublayers of the PHY, and their interfaces. The network architecture for 802.11g is setup using this toolbox. Value objects are used to organize properties required for generation of the 802.11g waveforms and to recover signal data from such waveforms such as modulation, channel bandwidth, PSDU length, number of transmit antennas, waveform format and packet recovery.

In the Communication System Toolbox, a binary data stream is generated. The message bits are encoded using Reed Solomon FEC method. BPSK modulation is applied to the encoded data. The modulated signal is passed through AWGN channel to add white gaussian noise. The received signal is demodulated by a BPSK Demodulator and passed on to the Reed Solomon Decoder for hard decision decoding. The system BER is calculated. The functions used during this process are as follows: `comm.RSEncoder`, `comm.RSDecoder`, `comm.BPSKModulator`, `comm.BPSKDemodulator`, `comm.AWGNChannel` and `comm.ErrorRate`.

The SimEvents library contains building blocks that model the MAC layer. The blocks have dialog boxes where you specify the desired parameters. For example, the Entity Server, serves entities, such as packets, as they arrive at the input. It can serve multiple packets simultaneously and output each packet through the output port. The outputs specify number of packets that entered the block, number of packets departed, number of packets pending and the average waiting time. Packet traffic arrives at the input using a Poisson Process. Figure 14 shows the representation of the WTSN.

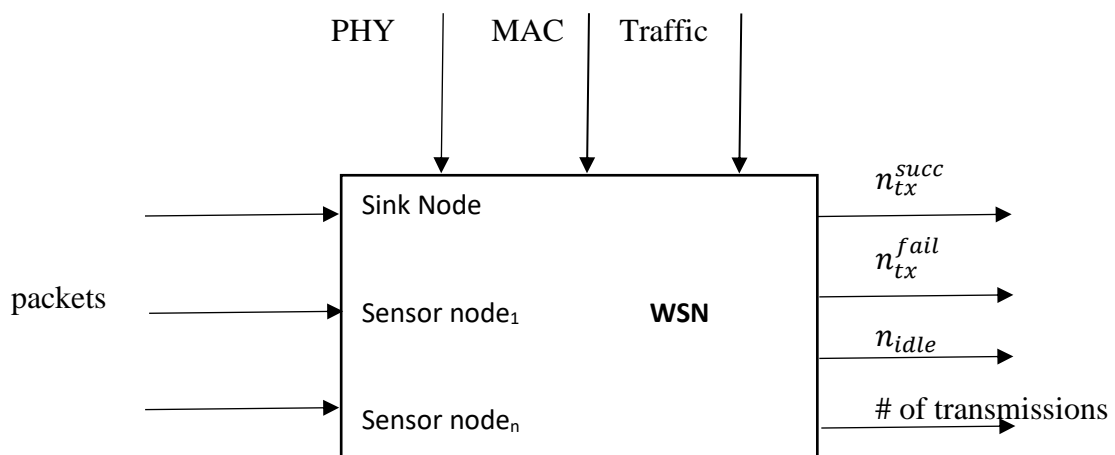


Figure 14: General Representation of WTSN Simulation

### 5.3 Simulation Details

The simulation involves the transmitting sensor nodes that send data packets through the communication channel to the receiving sink node. 802.11g channel is employed to assume the communication in the physical layer. The data signal is modulated using BPSK over a radio channel with maximum capacity of 1 Mbps. Models for functional blocks such as modulators, encoders, filters, amplifiers, and channels are used to simulate the flow of data packets where the system performance is measured with regard to the bit error rate performance, throughput and average delay for successful packet transmission and offered traffic load. Figure 14 shows the general representation of the WTSN. The PHY and MAC layer modules of the sensor nodes are required to have the ability to communicate with each other. The simulation model outputs the number of collisions, total number of transmitted packets and the number of idle slots spent during the transmission period. The bit error probability values calculated analytically were employed in the simulation model to evaluate the probability of successful transmission in the physical layer.

Two methods are used for verifying the precision of the models by comparing the simulation and analytical results in the following manner:

- (i) The Markov chain model results should tally with the simulation model with regards to the total number of steps to absorption.
- (ii) The analytical results should tally with the simulation results for a borderline setting scenario, where there are no new packet arriving during the competition period. These results relate to the expected number of transmissions needed to achieve absorption.

The Entity Generator block generates the entities. In this case the entities represent the data packets in the WTSN. Each node is modelled according to the M/M/1 queue following a Poisson arrival process to receive the packets. The data packets from each node are processed by a single server by the order of their arrival.

#### 5.4 Chapter Conclusion

In this chapter, the implementation of the prototype is outlined. In the next chapter, the simulation tests and test results are presented and analysed.

## CHAPTER SIX: SIMULATION TESTS AND RESULTS

### 6.1 Introduction

This chapter presents simulation test procedures and test results. The reasons for carrying out the tests are also outlined. The simulation was performed to analyse the possible energy gains that could be realised by optimising the FEC rate using different Reed Solomon codes and channel access probabilities.

### 6.2 Simulation Tests

To test the validity of the optimisation model, emphasis was placed on scrutinising the effect of forward error correction and probability of channel access on the energy utilisation of the network. This is because the key objective of this research study was to outline a cross-layer protocol that is energy efficient and optimises energy conservation of the network at the PHY and MAC layers. The values of the parameters applied in these computations are specified in Table 3 on page 48. These parameters are outlined closely ensuing the IEEE Standard 802.11 2012. The baseline case is the case with no forward error coding. The performance metrics that were used are:

- (i) Bit error probability.
- (ii) Packet success probability.
- (iii) Number of steps to absorption.
- (iv) Number of transmissions to absorption.
- (v) Time to absorption.
- (vi) Energy saving.

Table 4: Simulation Tests and Results Obtained

Test type	Description of test	Results
Test 1	Checking the effect of FEC scheme on the bit error probability of the PHY layer	The code rates which requires the lowest SNR for a given BEP is chosen as the optimum code rate.
Test 2	Analysing the effect of tuning PHY and MAC layers on packet success probability	PHY and MAC layer tuning affected the probability of successful packet transmission.
Test 3	Comparing the effect of optimisation on the number of steps to reach absorption.	There was a significant change in quantity of steps in response to optimisation.
Test 4	Evaluating the effect of tuning PHY and MAC layer on transmission time.	Time to absorption improved when coding was applied.
Test 5	Measuring energy savings for different RS code rates with probability to transmit set.	The scheme showed which code rates can save energy
Test 6	Comparing energy saving between two different MAC methods.	SMAC consumes less energy than S-ALOHA

### 6.2.1 Bit Error Probability

Applying Reed Solomon codes to the PHY layer produced the error performance of the transmission link regarding the ratio of energy per bit information to noise power spectral density ( $E_b/N_0$ ) was conducted. The results are presented in Table 5 and laid out in Figure 15.

Table 5: BEP Performance for Uncoded and Coded PHY Protocol

Eb/No	BEP Performance for Uncoded and Coded PHY Protocol							
	BEP case	Uncoded	BEP RS Code (63,57)	BEP RS Code (63,55)	BEP RS Code (63,53)	BEP RS Code (63,51)	BEP RS Code (63,49)	BEP RS Code (63,47)
4	0.02468		0.01491	0.01553	0.01604	0.01652	0.01708	0.01781
5	0.01743		0.00946	0.00914	0.00874	0.00837	0.00813	0.00807
6	0.01183		0.00487	0.00410	0.00343	0.00291	0.00256	0.00234
7	0.00769		0.00190	0.00130	0.00090	0.00064	0.00049	0.00040
8	0.00476		0.00054	0.00028	0.00015	8.88755e-05	5.60337e-05	3.91496e-05
9	0.00279		0.00011	4.16952e-05	1.66390e-05	7.33407e-06	3.65731e-06	2.09804e-06
10	0.00154		1.63676e-05	4.10390e-06	1.13793e-06	3.62322e-07	1.35893e-07	6.11199e-08
11	0.00079		1.72313e-06	2.70691e-07	4.90294e-08	1.06485e-08	2.84807e-09	9.56007e-10

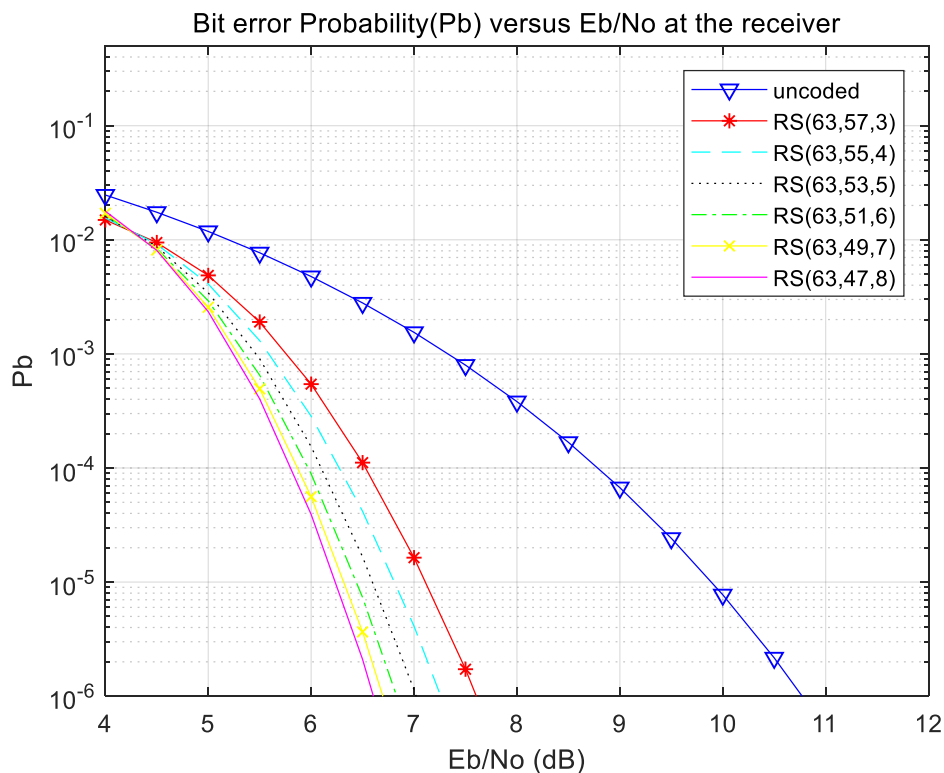


Figure 15: Bit Error Probability versus Signal to Noise Ratio in dB

The Reed Solomon codes are generated as a consequence of the 6-bit symbol employed. Depending on the redundancy bits applied, it gives rise to the (n,k) value. According to the graph, BEP decreases as  $E_b/N_0$  increases and when coding is applied BEP performance improves significantly.

## 6.2.2 Packet Success Probability

The probability of successful packet transmission over an AWGN channel is affected when tuning of the MAC layer is considered. The outcomes are presented in Table 6 and laid out in Figure 16.

Table 6: Comparison of Packet Success Probability

Eb/No	Packet Success Probability Before and After Optimisation					
	PHY, uncoded	PHY, 0.87	PHY, 0.78	PHY, uncoded & MAC	PHY, 0.87 & MAC	PHY, 0.78 & MAC
4	0.00039	0.26510	0.60525	0.00014	0.10003	0.22839
5	0.00780	0.74908	0.94465	0.00294	0.28266	0.35647
6	0.05816	0.95852	0.99629	0.02195	0.36170	0.37595
7	0.20802	0.99583	0.99986	0.07850	0.37578	0.37730
8	0.44470	0.99972	0.99999	0.16780	0.37724	0.37735
9	0.67846	0.99998	0.99999	0.25602	0.37734	0.37735
10	0.84308	0.99999	0.99999	0.31814	0.37735	0.37735
11	0.93395	0.99999	0.99999	0.35243	0.37735	0.37735
12	0.97569	0.99999	1	0.36818	0.37735	0.37735

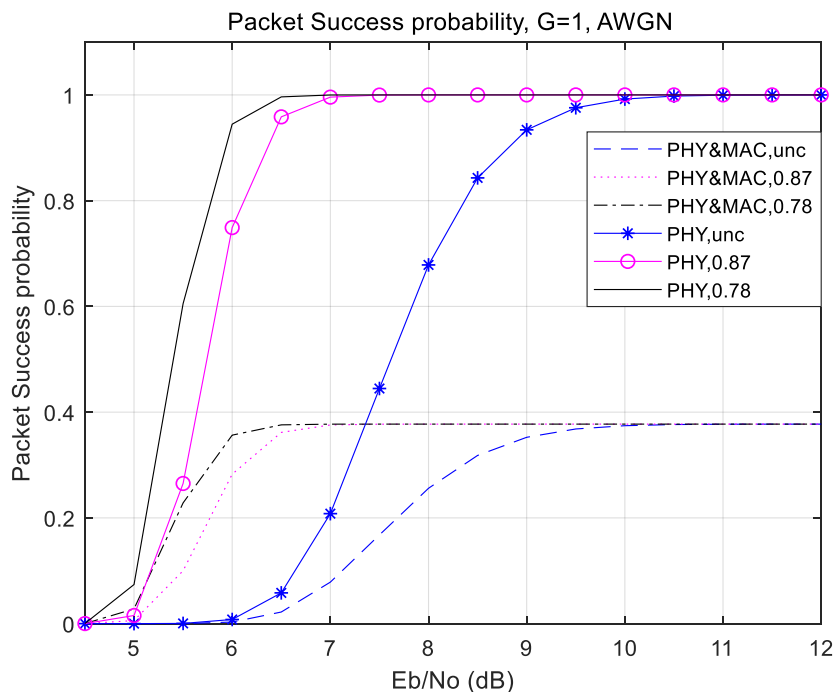


Figure 16: Packet success probabilities vs  $\frac{E_b}{N_o}$  in dB for uncoded and coded cases

The graph shows the effect of jointly tuning the PHY and MAC layer on packet success probability versus only tuning the PHY layer. Three sets of curves that cut off at 1 on the vertical axis represent optimisation of the PHY layer only while the second set of curves that cut off at 0.377 take the MAC layer into account. There is a significant drop in packet success probability when joint layer tuning is applied.

### 6.2.3 Number of Steps to Absorption

The Markov chain model was employed to calculate the number of steps to absorption, which indicate the value when every sensor node has transferred its packet successfully. In the simulation the same results were obtained. Table 7 presents the number of steps to absorption for the coded and uncoded cases. The results are presented for several channel competition probability values,  $p = 1/(M - j)$ ,  $p = 0.1$  and  $p = 0.05$  and are plotted in Figure 17. The value for the number of steps plotted was capped at 500 to provide a tidy graph.

Table 7: Number of Steps to Absorption

Eb/No	Number of Steps to Absorption					
	PHY, uncoded & p = 0.05	PHY, 0.87 & p = 0.05	PHY, uncoded & p = 0.1	PHY, 0.87 & p = 0.1	PHY, uncoded & p = 1/(M-j)	PHY, 0.87 & p = 1/(M-j)
4	186468	5211	69650	2075	19024	1612
5	25318	350	9482	165	2604	113
6	3509	108	1339	70	382	34
7	557	96	237	65	81	34
8	158	95	88	65	40	34
9	103	95	68	65	35	34
10	96	95	65	65	34	34
11	95	95	65	65	34	34
12	95	95	65	65	34	34

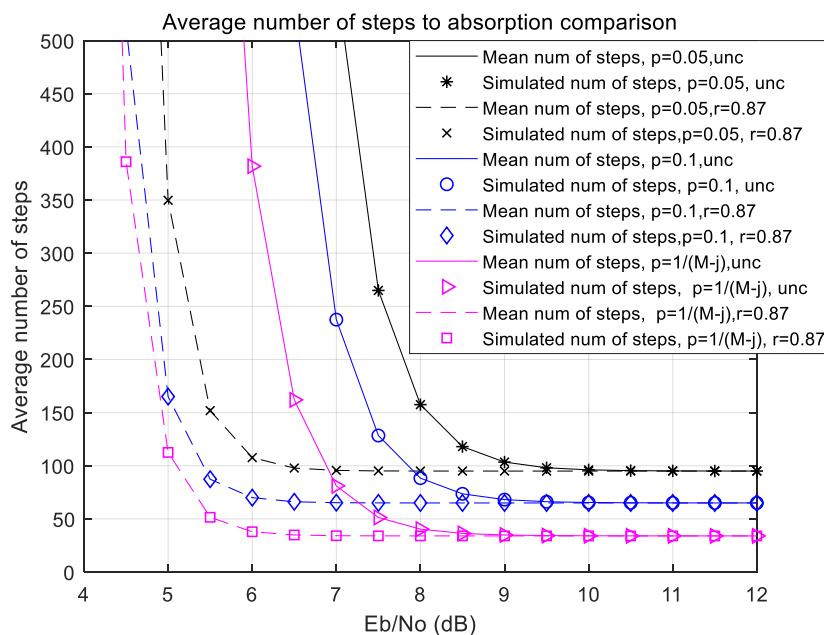


Figure 17: Average number of steps vs  $\frac{E_b}{N_o}$  in dB calculated using theoretical and simulation models with different p values.

The graph illustrates that the analytically calculated results tally with the simulated results. When coding is applied, the average number of steps to absorption is drastically reduced. Varying the channel competition probability shows a higher average number of steps for  $p = 0.05$  compared to  $p = 0.1$ . The channel probability  $p = 1/(M - j)$  presents the lowest mean number of steps.

### 6.2.4 Number of Transmissions to Absorption

The mean number of transmissions needed to achieve the state of absorption was computed applying Equation (39) and the results matched the simulation for each corresponding case. Table 8 presents the results which are plotted in Figure 18. The plot for number of transmissions was limited to 1000 to provide a clear graph.

Table 8: Number of Transmissions to Absorption

Eb/No	Number of Transmissions to Absorption					
	PHY, uncoded & p = 0.05	PHY, 0.87 & p = 0.05	PHY, uncoded & p = 0.1	PHY, 0.87 & p = 0.1	PHY, uncoded & p = 0.2	PHY, 0.87 & p = 0.2
4	3448	280	7023	557	190246	5603
5	204	46	1007	89	26043	1055
6	42	35	192	66	3821	439
7	34	34	82	65	814	356
8	34	34	67	65	407	345
9	34	34	65	65	352	343
10	34	34	65	65	344	343
11	34	34	65	65	344	343
12	34	34	65	65	344	343

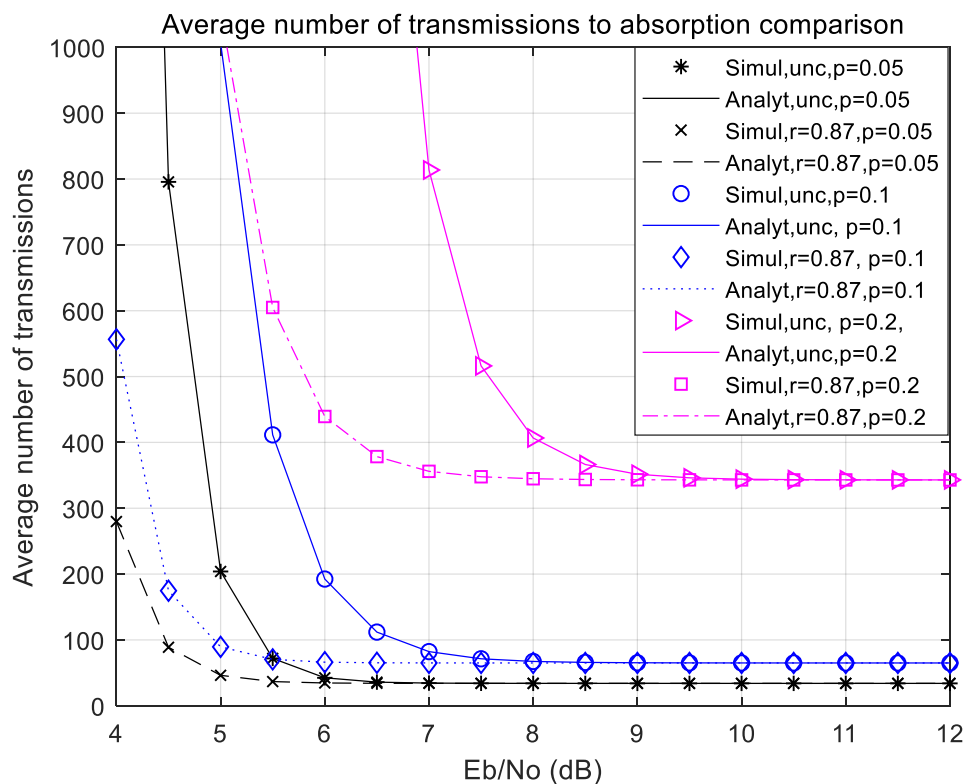


Figure 18: Analytical and simulation results of average number of transmissions requisite to attain absorption state.

In the above figure the number of transmissions to absorption is optimal when  $p = 0.05$ . It also shows that at certain  $E_b/N_0$  values coding ceases to make a difference in the number of transmissions to absorption required.

### 6.2.5 Time to Absorption

A comparison of the percentage improvement in time to absorption for uncoded transmission with the different code rates was done using Equation (33), the Markov chain model. A calculation of the improvement in percentage form was done comparing the different code rates to the uncoded case and the results are presented in Table 9 and laid out in Figure 19.

Table 9: Percentage Saving on Average Number of Steps

Eb/No	Percentage Saving on Average Number of Steps				
	r=0.97	r=0.90	r=0.87	r=0.81	r=0.78
4	-	55.5019	66.54574	34.28673	0
5	36.46878	72.23862	74.23862	80.25850	78.0159
6	22.29369	45.56166	43.6548	48.50241	44.30299
7	9.19599	17.927	17.927	19.927	17.92464
8	2.97501	5.71506	5.71506	5.71506	5.44585
9	0.85302	1.62311	1.62311	1.82311	1.64821
10	0.38694	0.78403	0.78403	0.88403	0.73837
11	0.13614	0.24063	0.24063	0.29063	0.23497
12	0.00112	0.002	0.002	0.002	0.002

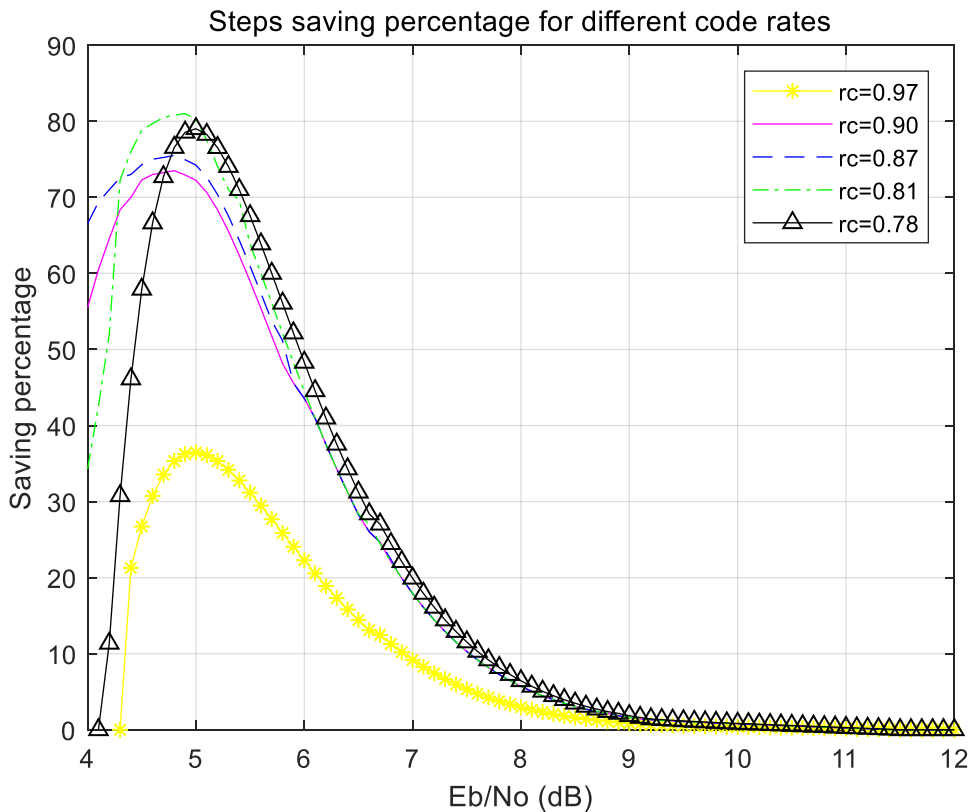


Figure 19: Saving percentage in average number of steps versus Eb/No in dB for different code rates,  $p=0.05$ .

The results in Figure 19 show that in comparison to the uncoded case, the least efficient code rate  $r = 0.97$ , provided the highest energy gain of 36%. The most efficient code rate is  $r = 0.81$  producing the highest energy saving of 81%.

The results in Table 10 are plotted in Figure 20 and are computed by applying Equation (35) in section 4.9. It shows the percentage gains for different code rates for time to absorption comparing with the case with no coding.

Table 10: Transmission Time Saving Percentage

Eb/No	Transmission Time Saving Percentage				
	r = 0.97	r = 0.90	r = 0.87	r = 0.81	r = 0.78
4	-	50	61	20	-
5	36.018	69.6019	73.23862	77	74.54372
6	33.5401	55.15450	56.07205	56.1545	52.15450
7	21.8580	23.4665	23.46658	26.1018	21.10188
8	8.9381	7.17043	6.170435	6.06142	4.26160
9	2.3894	0	-	-	-
10	0.6187	-	-	-	-

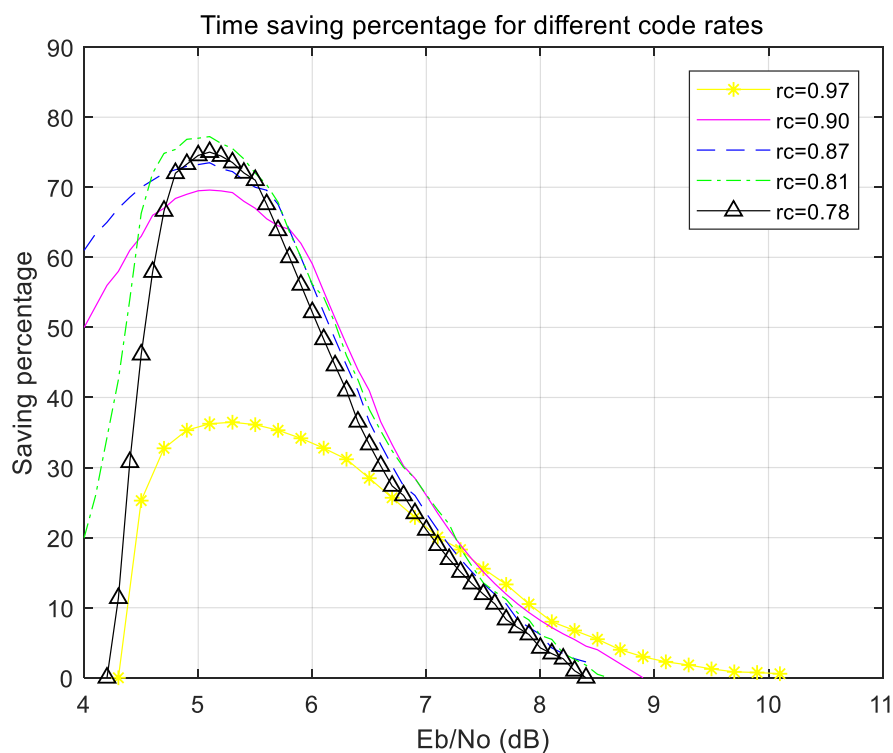


Figure 20: Average time saving percentage versus Eb/No in dB for different code rates,  $p=0.05$ .

The results in Figure 20 show that the maximum time to absorption saving is 77,2% obtained when  $r = 0.81$  at 5.1dB. The least gain occurs when the code rate  $r = 0.97$ . The time to absorption savings reaches zero at lower Eb/No values compared to the steps to absorption savings in Figure 19.

### 6.2.6 Energy Saving

The percentage saving in energy for distinct coding rates in contrast with the energy saving in the transmission of the uncoded case was calculated in this instance. The most energy-efficient code rate could be determined. The results are presented in Table 11 and laid out in Figure 21.

Table 11: Energy Saving Percentage

Eb/No	Energy Saving Percentage				
	r = 0.97	r = 0.90	r = 0.87	r = 0.81	r = 0.78
4	0	45	56	20	0
5	31.25095	64.5	68.23862	72	70.54372
6	27.7728	54.07205	52.07205	56.15450	48.15450
7	14.07131	23.02485	21.46658	26.10188	17.10188
8	1	5.18131	4.17043	6.0614	1.26160
9	0	0	-	-	0

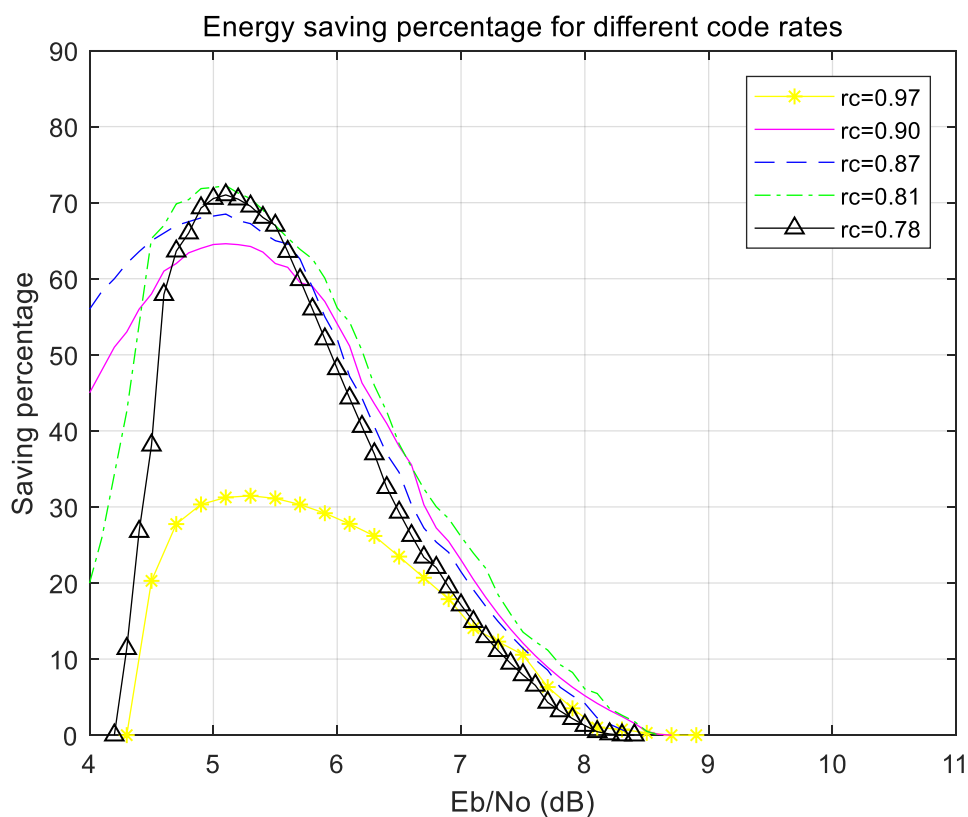


Figure 21: Percentage energy saving result vs  $\frac{E_b}{N_o}$  in dB when using different code rates,  $p = 0.05$ .

Figure 21 shows that the least energy efficient rate is  $r = 0.97$  while the most efficient code rate is  $r = 0.81$  with energy savings of 72%. The energy savings reach zero at lower  $E_b/N_o$  values than the time to absorption savings in Figure 20.

### 6.2.7 Comparison of MAC Methods

Consumption of energy of the S-Aloha and SMAC media access control protocols in combination with AWGN channel provides. Equation (44) in, section 4.11, is used to calculate these results. Table 12 presents the results and plotted in Figure 22.

Table 12: Comparison of MAC Methods Energy Consumption in Joules

Eb/No	Comparison of MAC Methods Energy Consumption in Joules							
	SALOHA, uncoded	SMAC, uncoded	SALOHA, r = 0.97	SMAC, r = 0.97	SALOHA, r = 0.87	SMAC, r = 0.87	SALOHA, r = 0.78	SMAC, r = 0.78
4	0.14578	0.09067	0.40829	0.21735	0.94357	0.59715	0.98669	0.39889
5	0.10367	0.06394	0.24839	0.13200	0.42535	0.24352	0.45130	0.18884
6	0.07389	0.04513	0.15140	0.08024	0.19250	0.09975	0.20709	0.08962
7	0.05283	0.03190	0.09257	0.04884	0.08787	0.04129	0.09571	0.04275
8	0.03794	0.02259	0.05690	0.029804	0.04086	0.01753	0.04490	0.02062
9	0.02741	0.01604	0.03525	0.01825	0.01973	0.00786	0.02173	0.01016
10	0.01997	0.01143	0.02213	0.01124	0.01024	0.00394	0.01116	0.00522
11	0.01470	0.00819	0.01417	0.00699	0.00597	0.00234	0.00634	0.00288
12	0.010982	0.00591	0.00934	0.00442	0.00406	0.00169	0.00414	0.00178243

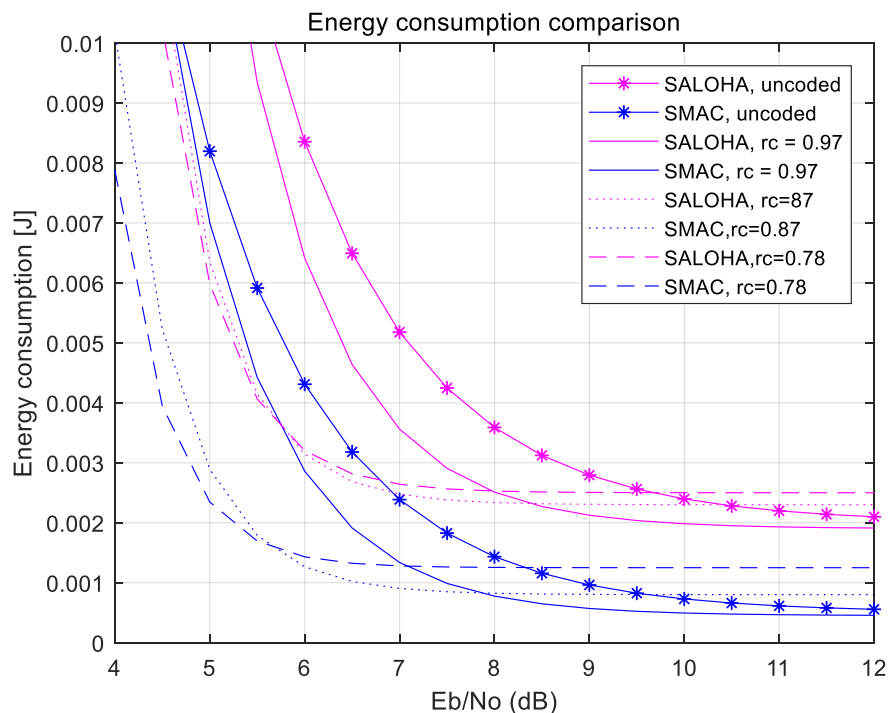


Figure 22: Comparison of energy consumption between S-Aloha and SMAC Medium Access protocols.

Figure 22 shows that SMAC outclasses S-Aloha in energy saving performance. However, the percentage savings for Eb/No values greater than 8.5dB drops significantly for SMAC compared to S-Aloha.

### 6.3 Chapter Conclusion

In Chapter 6, I gave an outline of the simulation test procedures. A presentation of the results obtained in the simulations was laid out. The next chapter analyses these results.

## CHAPTER SEVEN: ANALYSIS OF TEST RESULTS

### 7.1 Introduction

This chapter provides the analysis of the results obtained from the simulation tests in the endeavour to establish if the proposed solution functioned as designed and the research objectives were achieved.

### 7.2 Bit Error Probability

The expression of bit error rate on the AWGN channel was obtained in reference to the ratio of energy per bit to the single sided noise power spectral density,  $E_b/N_0$ . Coding of the PHY layer introduced extra bits to the data frame, resulting in the reduction of information bits in order to accommodate the redundancy since the length of the data packets is fixed. The performance of the transmission link was evaluated in terms of  $E_b/N_0$ . According to the results in Figure 15, to achieve the desired BER of  $10^{-5}$  the uncoded system required 9.9dB energy per transmitted bit, while the coded scenario resulted in the value reducing to as low as 6.2dB for the RS code 0.75. This is referred to as coding gain, and shows that, for the same performance without coding, the system consumes less energy when coding is applied. Although there is code gain with lower code rates, the rate of code gain decreases as the code rate decreases. This results in a cut-off region where reducing the rate any further does not improve the code gain. The RS codes employed were such that the block length was constant with varied redundancy. According to the performance curve, as the redundancy increases from 3 to 8 the code rate decreases resulting in the BER performance improving, because the error codes become more efficient, thus improving the probability of physical channel access  $P_{succ}^{PHY}$  as shown in Figure 15.

### 7.3 Packet Success Probability

Packet success probability in wireless networks is the probability of packets being successfully received at the sink node. For an ideal receiver, the MAC layer analysis traditionally does not consider the effect of the probability of transmission in the PHY layer as it is assumed to be one. In this body of work, joint success probability, which incorporates the effects of PHY and MAC layers together, was considered. Figure 16 illustrates the difference between the coded and uncoded scenarios, where the coded case assumes  $r = \{0.87, 0.78\}$  and reflects the impact of joint probability. The curves in Figure 16 labelled “PHY and MAC” at the maximum value one, correspond to the ideal receiver.

Similarly, in the studies of the PHY layer, consideration of the probability of successful channel access in the MAC layer is not considered and is assumed to be one. This corresponds to the curves labelled “PHY”. The results in Figure 16 indicate that, there is a transition state that exists between zero and maximum, within certain values of Eb/No, where the joint success probability of  $P_{succ}^{PHY}$  and  $P_{succ}^{MAC}$  do not guarantee communication that is error-free at the PHY layer. The results also show that, when  $P_{succ}^{PHY} = 1$ , that is, the error-free region of the PHY layer, the combined packet success probability is 0.368 nonetheless, owing to the S-Aloha MAC characteristics. These results highlight the importance of considering both the MAC and PHY layer probabilities of success.

#### 7.4 Number of Steps to Absorption

The Markov chain model was applied to determine the number of steps needed for each node in the WTSN to report its contents to the sink node successfully. The number of steps to absorption is important because it was then converted into time to absorption after finding the length of each step. Knowledge of the time to absorption allowed for the assessment of the consequence of optimising the physical and MAC layers.

According to the results obtained, the Markov chain model and the MATLAB simulation produce the identical results on the average number of steps required to attain absorption as shown in Figure 17. In addition, these results show the effect of the channel competition probability on the average steps to absorption. It can be observed that  $p = 0.1$  has a lower number of average steps to absorption compared to  $p = 0.05$ . This is because, the latter has less nodes competing in the channel because of the smaller probability and will therefore have more idle steps. The optimum  $p$  value depends on the number of nodes taking part in the channel competition. In this research, when the competition period initially begins, the number of nodes contending for a slot,  $M = 20$  and the optimal probability to transmit in this slot,  $p = 0.05$  for the S-Aloha media access control protocol. Nevertheless, during this period of competition the competing nodes decrease in number when nodes begin to transmit and the channel probability of  $p = 0.05$  becomes too small. In figure 16, the observation is that, for the case when  $G = 1$ , traffic load is at its optimal for such a network and the average number of steps is minimised where  $p = 1/(M - j)$ .

## 7.5 Number of Transmissions to Absorption

For the analytical results, the average number of transmissions required to achieve the absorption state took into consideration the average number of steps needed for a node to successfully transmit as well as the expected number of transmissions occurring for the duration of a step. This set of results was compared to the output of the simulation model for each corresponding case. The results obtained from the simulation correspond with the analytically calculated results for the average number of transmissions as shown in Figure 18. This gives certainty to the adoption of this simulation model for the circumstances that might not be verifiable analytically. The results in Table 8 show that when the probability of channel competition is at its lowest,  $p = 0.05$ , a smaller number of transmissions is needed to achieve absorption. This is because there will be less collisions during the competition period as the chances of accessing the channel are lower. The probability of channel access  $p = 0.2$  is on the high extreme. It results in a drastic increase in the number of transmissions during the period of competition for the slots. It is similarly observed that the instance with uncoded transmission when  $p = 0.05$  requires even fewer transmissions to attain absorption compared to the coded instance when  $p = 0.1$  for values of  $E_b/N_0$  greater than 5.5dB. These results illustrate the cross-layer trade-off which is reliant on the attributes of the PHY and MAC layers as they have a bearing on the type of results obtained.

## 7.6 Transmission Time Saving

Optimising the physical and MAC layer reduces the number of steps needed for the nodes to transmit their packets to the sink node. The results in Figure 19 indicate that the maximum saving can be as high as 81% at  $E_b/N_0$  4.9dB for the code rate  $r = 0.81$ . When the number of symbols for error correction is small, for example, when  $r = 0.97$ , the error correction capability is also low, and therefore results in more steps to absorption. This results in a lower percentage gain as shown in the graph.

Tuning the coding rate for error correction reduced the number of retransmissions and thus shortened the length of the transmission period. This has a ripple effect on the time to absorption as it depends on the length of the transmission period for its determination. Figure 20 shows the percentage gains for different code rates for time to absorption comparing with the case with no coding. The redundancy generated by the code rate increases the duration of the data frame and hence a longer slot length, but it also reduces retransmission rate. Low code rates result in high coding redundancy thus making the length of the slot duration inefficient.

The results show that savings in time to absorption up to 77% are possible and decline to zero at lower values of  $E_b/N_0$  compared to the savings for average steps to absorption in Figure 19. The results show that the percentage saving for time could be manipulated upwards with the right code rate for a specific  $E_b/N_0$  value.

### 7.7 Energy Saving

The results from Figure 17 and 18 verified that the simulation model matched the theoretical and analytical results. This meant that the outputs obtained from the simulation, namely, the number of idle slots, retransmissions and collisions, could be used in the calculations for energy consumption. The energy saving percentage for distinct code rates is shown in Figure 21, in contrast to the transmission of the uncoded case. Figure 21 shows that when  $r = 0.81$ , that is the code rate which produces maximum energy efficiency, could contribute the energy savings of around seventy nine percent. The weakest code rate  $r = 0.97$ , could contribute savings of a maximum of 36%. The difference in energy savings between these two code rates is significant because of the amount of retransmissions experienced at code rate  $r = 0.97$ , which consumes more energy. However, it can be observed that this code rate offers energy gains for the broadest range of  $E_b/N_0$  values compared to the other code rates. When the  $E_b/N_0$  is greater than 8.5dB the performance for the code rate  $r = 0.97$  performs more proficiently than the other cases. The results show that for  $E_b/N_0$  values smaller than 8.5dB, the stronger code rates should be employed as they deliver better energy savings.

Comparing the percentage savings on the number of steps (Figure 20), and the energy saving percentage (Figure 21), there is a concrete conjunction between the mean number of steps to absorption and the amount of energy saved. This is because there is a relationship between the average number of steps to absorption and the required average number of transmissions, being the principal source of energy depreciation in the network. With these results it may be concluded that the derivations that were analytically obtained to calculate the mean number of transmissions for absorption and the Markov chain model can produce a consistent interpretation on which code rates may save energy.

It can be deduced from the results that the  $E_b/N_0$  range of values that lead to energy preservation is constricted. This is because, for an elementary receiver architecture used in this research, the hard decision decoding used in the FEC method, yields a maximum coding gain of approximately 3dB. This value produces a difficulty for a fast and accurate estimation of the

channel that must be employed to aid changes in adaptive code rates. The computational capabilities of the sensor nodes do not provide for that essential level of estimation. The RS coding used in this research together with the model provide an instrument to optimise energy conservation by tuning the Reed Solomon codes.

## 7.8 Comparison of MAC Methods

The results for consumption of energy of the S-Aloha and SMAC media access control protocols in combination with AWGN channel are shown in Figure 22. Equation (44) in section 4.11, was used to calculate these results. In reference to the SMAC protocol, the assumption was that there is perfect synchronisation between the sink node and the sensor nodes, and thus their transmission slots schedule, which would lead to channel access which is collision free. In reference to S-Aloha, the assumption is that there is an optimal slot transmission probability, namely,  $p = 1/(M-j)$  for the node. The results show that SMAC surpasses S-Aloha since there aren't any collisions during the competition period, resulting in fewer retransmissions and therefore less energy consumption.

For  $E_b/N_0$  values greater than 8.5dB it can be stated that SMAC would lead to almost fifty percent lesser consumption of energy compared to exploiting the S-Aloha protocol. For specific  $E_b/N_0$  values, however, the results show that if strong coding is combined with the S-Aloha protocol, it will lead to decreased energy depletion as compared to a SMAC protocol with weak coding. For example, at  $E_b/N_0 = 5.6$ dB, code rates  $r = 0.87$  or  $r = 0.78$  for S-Aloha delivers lower energy utilisation than SMAC with code rate  $r = 0.97$  or when compared with the uncoded PHY layer transmission. Considering that SMAC would entail a bigger control overhead compared to S-Aloha, the variance in energy consumption would be greater in a real-world implementation. The straightforward contrast between S-Aloha and SMAC coupled with AWGN and diverse code rates for error correction, highlight the fact that efficient energy consumption depends on the combined settings of the PHY layer features and the MAC layer attributes.

## 7.9 Chapter Conclusion

In this chapter, the simulation test results were evaluated in depth and the feasibility of the proposed solution was reviewed. The following chapter wraps up the dissertation by underscoring the findings, challenges and contributions, and proposes further work which could improve the proposed solution.

## CHAPTER EIGHT: CONCLUSION

### 8.1 Introduction

This chapter winds up the dissertation. A brief summary of the proposed solution and its performance is presented, the implications and applications of the research and recommendations for further work are specified. A scheme that saves energy and that can be deployed in wireless sensor networks, was propositioned, outlined, simulated and its performance evaluated. A cross-layer protocol was introduced to improve wireless communication by optimising the protocol layers responsible for communication. The joint performance of PHY and MAC layers is analysed using forward error correction and stochastic techniques respectively and the improvements of the cross-layer optimisation scheme quantified.

### 8.2 Implications of the Research

The suggested model was employed to assess the energy efficiency of various Reed Solomon coding rates for a Wireless Temperature Sensor Network using Additive White Gaussian Noise transceivers and S-Aloha Media Access Control. The approach considered the applicable attributes of the PHY and MAC layers that facilitate joint optimisation. This cross-layer scheme could also be utilised for the analysis of energy efficiency of other combinations of PHY and MAC protocols. This research study used SMAC to compare the energy efficiency of the two different MAC protocols. The results obtained from this research showed that by choosing the appropriate code rate for the PHY layer and channel specifications for the MAC layer, substantial savings in energy could be accomplished. Within specific settings in this research, the energy gains were over 75% for a specific code rate in comparison to the circumstance where no coding was applied. On the other hand, according to the results, there are some instances where applying a code rate does not result in energy saving, in comparison to the case where no coding is used.

### 8.3 Applications of the Research

The proposed optimisation model in this research can be used at the network implementation phase for code rate selection or can be computed adaptively during runtime with the right technology, that is, sensor nodes with strong computational capabilities. If the probable channel conditions are identified, the optimum code rate could be determined at the network planning

stage. The model could also be utilised for assorted error coding schemes or to investigate the effect of transmission power or the modulation on the cross-layer operation.

#### 8.4 Recommendations for Further Work

In this research, hard decision decoding was implemented for the error correction, but soft decision decoding of the Reed Solomon codes can be included in this model, as it can give larger coding gains for the AWGN channel case. However, deriving BEP and the energy consumption model would need to be revised for the improvements on the efficiency of the energy consumption to be verified. Other forward error correction methods could be explored in future work. In this research a star network topology was used, future work could explore other topologies that use clusters, as the sink nodes can connect with other sink nodes to form a hierarchical network. In this research stationary nodes were assumed, future work could explore mobile sensor nodes.

#### 8.5 Conclusion

In this research all the objectives were met. A cross-layer scheme was designed and implemented that provided energy savings in the WTSN. An analysis of the existing energy saving solutions was completed. An evaluation and comparison of possible energy savings was accomplished by jointly enhancing the PHY and MAC layers using the Markov chain model.

## REFERENCES

1. Karl H, Willig A. *Protocols and Architectures for Wireless Sensor Networks*. Chichester: Wiley; 2011.
2. Akyildiz I, Sankarasubramaniam Y, Cayirci E. A Survey on Sensor Networks. *IEEE Communications Magazine*, vol 40, no. 8, pp. 102-114, 2002.
3. Alkhatib A, Baicher G. MAC Layer Overview for Wireless Sensor Networks. *International Conference on Computer Networks and Communication Systems*. Singapore: IACSIT Press, pp. 16-19, 2012.
4. Babulal K, Tewari R. Cross Layer Design for Cooperative Transmission in Wireless Sensor Networks. *Wireless Sensor Network*, vol 3, no. 6, pp. 209-214, 2011.
5. Harish I, Sambasivan S. Protocol Stack Design and Implementation of Wireless Sensor Network for Emerging Application. *IEEE International Conference on Emerging Trends in Computing, Communication and Nanotechnology*. Tirunelveli, India: IEEE, pp. 523-527, 2013.
6. Korger U, Hartmann C, Kusume K, Widmer J. Quality of Service Implications of Power Control and Multi-user Detection-based Cross-layer Design. *EURASIP Journal on Wireless Communications and Networking*, vol 1, no. 9, 2011.
7. Jagadeesan S, Parthasarathy V. Cross-Layer Design in Wireless Sensor Networks. In: Wyld D, Zizka J, Nagamalai D, ed. by. *Advances in Computer Science, Engineering & Applications Advances in Intelligent and Soft Computing*. Berlin, Heidelberg: Springer: pp. 283-295, 2012.
8. Charfi W, Masmoudi M, Derbel F. A Layered Model for Wireless Sensor Networks. *2009 6<sup>th</sup> International Multi-Conference on Systems, Signals and Devices*, Djerba, Tunisia: IEEE, pp. 1-5, 2009.
9. Fahmy H.M.A. Protocol Stacks of WSNs. In: *Wireless Sensor Networks*, Singapore: Springer: pp. 55-68, 2016.
10. Poellabauer C, Dargie W. *Fundamentals of Wireless Sensor Networks*. 2nd ed. Hoboken, N.J.: Wiley; 2013.
11. Chen Z, Li S. An Energy-Efficient Access Control Algorithm with Cross-Layer Optimization in Wireless Sensor Networks. *Wireless Sensor Network*, vol 2, no. 2, pp. 168-172, 2010.
12. Charan P, Paulus R, Kumar M, Jaiswal A. A Cross Layer Approach for Performance Optimisation in Wireless Sensor Networks using Cooperative Diversity. *International Journal of Computer Science & Technology*, vol 3, no. 2, pp. 158-163, 2012.
13. Li M, Jing Y, Li C. A Robust and Efficient Cross-Layer Optimal Design in Wireless Sensor Networks. *Wireless Personal Communications*, vol 72, no. 4, pp. 1889-1902, 2013.
14. Chao H, Chang C, Chen C, Chang K. Survey of Cross Layer Optimisation Techniques for Wireless Networks. In: Khosrow-Pour M, Clarke S, Jennex M, Becker A, Anttiroiko A, ed. by. *Wireless Technologies: Concepts, Methodologies, Tools and Applications*. Hershey, New York: IGI Global, pp. 60-76, 2012.
15. Shabdanov S, Mitran P, Rosenberg C. Cross-Layer Optimization Using Advanced Physical Layer Techniques in Wireless Mesh Networks. *IEEE Transactions on Wireless Communications*, vol 11, no. 4, pp. 1622-1631, 2012.
16. Fu B, Xiao Y, Deng H, Zeng H. A Survey of Cross-Layer Designs in Wireless Networks. *IEEE Communications Surveys & Tutorials*, vol 16, no. 1, pp. 110-126, 2014.
17. Proakis J, Salehi M. *Communication Systems Engineering*. 2nd ed. New Jersey: Prentice Hall; 2002.
18. Tanenbaum A, Wetherall D. *Computer networks*. 5th ed. Boston: Pearson Education; 2011.

19. IEEE. IEEE Standard for Information Technology—Telecommunications and Information Exchange Between Systems—Local and Metropolitan Area Networks—Specific requirements Part II: wireless LAN medium access control (MAC) and physical layer (PHY) specifications IEEE Std 802.11g. IEEE. 2007.
20. Yick J, Mukherjee B, Ghosal D. Wireless Sensor Network Survey. *Computer Networks*, vol 52, no. 12, pp. 2292-2330, 2008.
21. Wang A, Chao C, Sodini C, Chandrakasan, A. Energy Efficient Modulation and Mac for Asymmetric RF Microsensor System. *Proceedings of the 2001 International Symposium on Low Power Electronics and Design*. Huntington Beach, California: IEEE, pp. 106-111, 2001.
22. Shuguang Cui, Goldsmith A, Bahai A. Energy-constrained Modulation Optimization. *IEEE Transactions on Wireless Communications*, vol 4, no. 5, pp. 2349-2360, 2005.
23. Deng J, Han Y, Chen P, Varshney P. Optimal Transmission Range for Wireless Ad Hoc Networks Based on Energy Efficiency. *IEEE Transactions on Communications*, vol 55, no. 9, pp. 1772-1782, 2007.
24. Holland M, Wang T, Tavli B, Seyedi A, Heinzelman W. Optimizing Physical-layer Parameters for Wireless Sensor Networks. *ACM Transactions on Sensor Networks*, vol 7, no. 4, pp. 1-20, 2011.
25. Modiano E. An Adaptive Algorithm for Optimizing the Packet Size Used in Wireless ARQ Protocols. *Wireless Networks Journal*, vol 5, no.4, pp. 279–286, 1999.
26. Ci S, Sharif H, Nuli K. Study of an Adaptive Frame Size Predictor to Enhance Energy Conservation in Wireless Sensor Networks. *IEEE Journal on Selected Areas in Communications*, vol 23, no. 2), pp. 283-292, 2005.
27. Hou Y, Hamamura M, Zhang M. 'Performance Tradeoff with Adaptive Frame Length and Modulation in Wireless Network'. *The Fifth International Conference on Computer and Information Technology*. Shanghai, China: IEEE, pp. 490-494, 2005.
28. Sankarasubramaniam Y, Akyildiz I, McLaughlin S. 'Energy Efficiency Based Packet Size Optimisation in Wireless Sensor Networks. *Proceedings of the First IEEE International Workshop on Sensor Network Protocols and Applications*. Anchorage, AK, USA: IEEE, pp. 1-8, 2003.
29. Ye W, Heidemann J, Estrin D. An Energy-Efficient MAC Protocol for Wireless Sensor Networks. *Twenty-First Annual Joint Conference of the IEEE Computer and Communications Societies*. IEEE, pp. 1567-1576, 2006.
30. van Dam T, Langendoen K. An Adaptive Energy-efficient MAC Protocol for Wireless Sensor Networks. *Proceedings of the 1st International Conference on Embedded Networked Sensor Systems*. Los Angeles, California: ACM, pp. 171-180, 2003.
31. Jamieson K, Balakrishnan H, Tay Y. Sift: A MAC Protocol for Event-Driven Wireless Sensor Networks. In: Römer K, Karl H, Mattern F, ed. by. *Lecture Notes in Computer Science*, vol 3868. Berlin, Heidelberg: Springer, pp. 260-275, 2006.
32. Enz C, El-Hoiydi A, Decotignie J, Peiris V. WiseNET: An Ultra-low Power Wireless Sensor Network Solution. *Computer*, vol 37, no. 8, pp. 62-70, 2004.
33. Rajendran V, Obraczka K, Garcia-Luna-Aceves J. Energy-Efficient, Collision-Free Medium Access Control for Wireless Sensor Networks. *Wireless Networks*, vol 12, no. 1, pp. 63-78, 2006.
34. Polastre J, Hill J, Culler D. Versatile Low Power Media Access for Wireless Sensor Networks. *Proceedings of the 2nd international conference on Embedded networked sensor systems*. Baltimore, MD, USA: ACM, pp. 95-107, 2004.
35. Jurdak R. *Wireless ad hoc and sensor networks: A Cross-Layer Design Perspective*. New York: Springer Science + Business Media, 2007.

36. Vuran M, Akyildiz I. XLP: A Cross-Layer Protocol for Efficient Communication in Wireless Sensor Networks. *IEEE Transactions on Mobile Computing*, vol 9, no. 11, pp. 1578-1591, 2010.
37. Mendes L, J.P.C. Rodrigues J. A Survey on Cross-layer Solutions for Wireless Sensor Networks. *Journal of Network and Computer Applications*, vol 34, no. 2, pp. 523-534, 2011.
38. Kulkarni S, Iyer A, Rosenberg C. An Address-light, Integrated MAC and Routing Protocol for Wireless Sensor Networks. *IEEE/ACM Transactions on Networking*, vol 14, no. 4, pp. 793-806, 2006.
39. Shu T, Krunz M. Energy-efficient Power/rate Control and Scheduling in Hybrid TDMA/CDMA Wireless Sensor Networks. *Computer Networks*, vol 53, no. 9, pp. 1395-1408, 2009.
40. Choi J, Kim H, Baek I, Kwon W. Cell Based Energy Density Aware Routing: A New Protocol for Improving the Lifetime of Wireless Sensor Networks. *Computer Communications*, vol 28, no. 11, pp. 1293-1302, 2005.
41. Aron F, Olwal T, Kurien A, Odhiambo M. Energy Efficient Topology Control Algorithm for Wireless Mesh Networks. *International Wireless Communications and Mobile Computing*. Crete Island, Greece: IEEE, pp. 135-140, 2008.
42. Yuan Y, Yang Z, He Z, He J. An Integrated Energy Aware Wireless Transmission System for Qos Provisioning in Wireless Sensor Network. *Computer Communications*, vol 29, no. 2, pp. 162-172, 2006.
43. Safwati A, Hassanein H, Mouftah H. Optimal Cross-Layer Designs for Energy-Efficient Wireless Ad Hoc And Sensor Networks. *Proceedings of the 2003 IEEE International Performance, Computing, and Communications Conference*. Phoenix, AZ, USA,: IEEE, pp. 123-128, 2003.
44. Suh C, Koh Y, Son D. An Energy Efficient Cross-Layer MAC Protocol for Wireless Sensor Networks. In: Shen T, Li J, Li M, Ni J, Wang W, ed. by. *Lecture Notes in Computer Science*, vol 3842. Berlin, Heidelberg: Springer; 2006.
45. Madan R, Shuguang Cui, Lall S, Goldsmith A. Modeling and Optimization of Transmission Schemes in Energy-Constrained Wireless Sensor Networks. *IEEE/ACM Transactions on Networking*, vol 15, no. 6, pp. 1359-1372, 2007.
46. Cui S, Madan M, Goldsmith A, Lall S. Joint Routing, MAC and Link Layer Optimization in Sensor Networks with Energy Constraints. *IEEE International Conference on Communications*. Seoul, South Korea: IEEE, pp. 725-729, 2005.
47. Akyildiz I, Vuran M, Akan O. A Cross-Layer Protocol for Wireless Sensor Networks. *40th Annual Conference on Information Sciences and Systems*. Princeton, NJ, USA: IEEE, pp. 1102-1107, 2006.
48. Bai Y, Liu S, Sha M, Lu Y, Xu C. An Energy Optimization Protocol Based on Cross-Layer for Wireless Sensor Networks. *Journal of Communications* vol 3, no. 6, pp. 27-34, 2008.
49. Karvonen H, Pomalaza-Ráez C, Hämmäläinen M. A Cross-Layer Optimization Approach for Lower Layers of the Protocol Stack in Sensor Networks. *ACM Transactions on Sensor Networks*, vol 11, no. 1, pp. 1-30, 2014.
50. Nguyen K, Nguyen V, Le D, Ji Y, Duong D, Yamada S. ERI-MAC: An Energy-Harvested Receiver-Initiated MAC Protocol for Wireless Sensor Networks. *International Journal of Distributed Sensor Networks*, vol 10, no. 5, pp. 1-8, 2014.
51. Mehta N, Murthy C. PHY and MAC Layer Optimization for Energy-harvesting Wireless Networks. In: Hossain E, Bhargava V, Fettweis G, ed. by. *Green Radio Communication Networks*. Cambridge: Cambridge University Press, pp. 53-77, 2012.

52. Olwal T, Van Wyk B, Kogeda P, Mekuria F. FIREMAN: Foraging-Inspired Radio-Communication Energy Management for Green Multi-Radio Networks. In: Khan S, Mauri J, ed. by. Green Networking and Communications: ICT for Sustainability. 1st ed. Boca Raton: CRC Press, pp. 49-62, 2013.
53. Bianchi G. Performance Analysis of the IEEE 802.11 Distributed Coordination Function. IEEE Journal on Selected Areas in Communications, vol 18, no. 3, pp. 535-547, 2000.
54. Zhang Y, He C, Jiang L. Performance Analysis of S-MAC Protocol under Unsaturated Conditions. IEEE Communications Letters, vol 12, no. 3, pp. 210-212, 2008.
55. Wang Y, Vuran M, Goddard S. Cross-Layer Analysis of the End-to-End Delay Distribution in Wireless Sensor Networks. IEEE/ACM Transactions on Networking, vol 20, no. 1, pp. 305-318, 2012.
56. Ma Y, Ma C. Introduction of FECs and its Applications on Internet & Wireless Communications. Advanced Materials Research, vol 403-408, pp. 1776-1780, 2012.
57. Lone F, Puri A, Kumar S. Performance Comparison of Reed Solomon Code and BCH Code over Rayleigh Fading Channel. International Journal of Computer Applications, vol 71, no. 20, pp. 23-26, 2013.
58. Ratnam D, SivaKumar S, Sneha R, Reddy N, Brahmanandam P, Krishna S. A Study on Performance Evaluation of Reed Solomon (RS) Codes Through an AWGN Channel Model in a Communication System'. International Journal of Computer Science and Communication, vol 3, no. 1, pp. 37-40, 2012.
59. Kumar S, Gupta R. Bit Error Rate Analysis of ReedSolomon Code for Efficient Communication System. International Journal of Computer Applications, vol 30, no. 12, pp. 11-15, 2011.
60. AbdelfatahAbdeltwab M, ElBarbary K, Elhenawy A. Performance Improvement of Coded OFDM Communication System in AWGN Channel. International Journal of Computer Applications, vol 110, no. 11, pp. 17-23, 2015.
61. Korrapati V, Prasad M, Reddy D, Tej G. A Study on Performance Evaluation of Reed Solomon Codes Through an AWGN Channel Model for an Efficient Communication System. International Journal of Engineering Trends and Technology, vol 4, no. 4, pp. 1038-1041, 2013.
62. Usha S, Nataraj K. BER Performance of Digital Modulation Schemes with and Without OFDM Model for AWGN, Rayleigh and Rician Channels. International Journal of Science and Research, vol 4, no. 11, pp. 330-335, 2015.
63. Xu D, Wang K. Stochastic Modeling and Analysis with Energy Optimization for Wireless Sensor Networks. International Journal of Distributed Sensor Networks, vol 10, no. 5, pp. 1-5, 2014.
64. Wang W, Vuran M, Goddard S. Stochastic Analysis of Energy Consumption in Wireless Sensor Networks. 7th Annual IEEE Communications Society Conference on Sensor, Mesh and Ad Hoc Communications and Networks. Boston, MA, USA: IEEE, pp. 1-9, 2010.
65. Ali Q. Simulation Framework of Wireless Sensor Network WSN Using MATLAB Simulink Software. In: Katsikis V, ed. by. MATLAB - A Fundamental Tool for Scientific Computing and Engineering Applications - Volume 2. Rijeka, Croatia: IntechOpen, pp. 264-286, 2012.
66. MATLAB R2018a [Internet]. Mathswork.com. 2018 [cited 15 June 2018]. Available from: <https://www.mathswork.com/>
67. Alsheikh M, Hoang D, Niyato D, Tan H, Lin S. Markov Decision Processes with Applications in Wireless Sensor Networks: A Survey. IEEE Communications Surveys & Tutorials, vol 17, no. 3, pp. 1239 – 1267, 2015.

68. Pinsky M, Karlin S. An Introduction to Stochastic Modelling. 4th ed. Burlington, MA, USA: Academic Press; 2011.
69. Freedman D. Markov Chains. 2nd ed. New York: Springer-Verlag; 1983.
70. Sweeney P. Error control coding. Chichester; New York: Wiley; 2005.
71. Yang O, Heitzelman W. Modeling and Throughput Analysis for SMAC with a Finite Queue Capacity. 2009 International Conference on Intelligent Sensors, Sensor Networks and Information Processing (ISSNIP), Melbourne, VIC, 2009, pp. 409-414.
72. Alejandra D, Luis J, Gonzalez-Mendez M. Wireless Channel Model with Markov Chains Using MATLAB. In: Katsikis V, ed. by. MATLAB - A Fundamental Tool for Scientific Computing and Engineering Applications - Volume 2. Rijeka, Croatia: IntechOpen, pp. 264-286, 2012.

## APPENDICES

### Appendix A: BEP.m

```
EbNo=(4:0.5:12)';
EbNoA=10.^(EbNo/10);
M=2;

%Phase shift keying requires differential encoding. Differential encoding
%prevents invasion of the signal and symbols respectively from affecting
%the data.

uncodedBER=berawgn(EbNo,'psk',M,'diff');

%Estimate the coded BER for BPSK with a (n,k) Reed Solomon code using hard
%decision decoding.

codedBERa=bercoding(EbNo,'RS','hard',63,61);
codedBERb=bercoding(EbNo,'RS','hard',63,59);
codedBERc=bercoding(EbNo,'RS','hard',63,57);
codedBERd=bercoding(EbNo,'RS','hard',63,55);
codedBERe=bercoding(EbNo,'RS','hard',63,53);
codedBERf=bercoding(EbNo,'RS','hard',63,51);
codedBERg=bercoding(EbNo,'RS','hard',63,49);
codedBERh=bercoding(EbNo,'RS','hard',63,47);

%Plot the BER curves%
semilogy(EbNo,uncodedBER,'b-v',EbNo,codedBERc,'r-*',EbNo,codedBERd,'c--',...
',...
EbNo,codedBERe,'k:',EbNo,codedBERf,'g-.',EbNo,codedBERg,'y-
x',EbNo,codedBERh,'m-')

xlabel('Eb/No (dB)')
ylabel('Pb')
legend('uncoded','RS(63,57,3)','RS(63,55,4)',...
'RS(63,53,5)', 'RS(63,51,6)', 'RS(63,49,7)', 'RS(63,47,8)')
grid

title('Bit error Probability(Pb) versus Eb/No at the
receiver','FontWeight','Normal')
axis([4 12 10^-6 0.5])
```

## Appendix B: PHYLayer.m

```
function P_succ = PHY_layer(Pb_i,b,tt,D)
% [P_succ] = PHY_layer(Pb,b,tt)
% [P_succ] - prob of successful transmission in the PHY layer
% [tt] - Redundant/parity bits: t = (2,3,4,5)
% [b] - Symbol length: 'b' bits per symbol
% [D] - Packet size
%
% 'b' MUST BE SET TO ZERO WHEN THERE IS NO CODING

if(b==0) % NO coding
    PEP_i = 1 - (1-Pb_i)^D;
else
% [Step 1:] %To calculate the symbol error probability before decoding
Psym.i
    Psyma_i = 1 - (1- Pb_i)^b;

% [Step 2:] Calculate decoded symbol error probability Pds.i
    Pds_i = CalcDecodeSymErrProb(tt,b,Psyma_i);

% [Step 3:] Calculate packet error probability PEPi from symbol error
probability
    n = 2^b-1;
    k = n-2*tt;
    ri = k/n;
    Di = D/ri;
    Xi = Di/b;
    PEP_i = 1 - (1 - Pds_i)^Xi;
end
% [Step 4:] Calculate prob of successful transmission in the PHY layer
P_succ = 1 - PEP_i;
```

## Appendix C: MarkovModel.m

```

function PM = GenerateTransitionMatrixEx(M)
    % Trans_Matrix = GenerateTransitionMatrix("#Nodes")
    % to generate say, 20 nodes simply execute 'P =
GenerateTransitionMatrix(20) '

    M=20;
%% Preliminaries
% <> Number of nodes with packets to transmit
N=M+1; % MATLAB indexes from 1 and not from zero
p=0.05; % probability to transmit in a slot
Pq=0.37; %P(a=0)=> 1-Pa probability that new packet does not arrive
Pa=1-Pq; % Probability that new packets arrive
PPHYsucc=0.9; % Physical layer success

%% Create the Markov matrix
PM = zeros(N,N);
PM(N,N) = 1;

for jj=1:M
    p=1/(N-jj)
    %LAST VALUE IN A ROW

    PM(jj,jj+1) = (M-jj+1)*p*(1-p)^(M-jj)*Pq^(jj)*PPHYsucc;

    if(jj>1)
        PM(jj,jj) = (M-jj+1)*p*(1-p)^(M-jj)*nchoosek(jj,1)*PPHYsucc*Pa*Pq^(jj-
1)+...
            (1-(M-jj+1)*p*(1-p)^(M-jj))*nchoosek(jj-
1,0)*PPHYsucc*Pa^0*Pq^(jj-1);
        end

    if(jj>2)% Begin at row 3
        for(m=2:jj)% Begin from the 2nd element
            kk = jj - m;
            alpha = (M-jj+1)*p*(1-p)^(M-jj);
            PM(jj,m) = alpha*nchoosek(jj, kk+1)*PPHYsucc*Pa^(kk+1)*Pq^(jj-
(kk+1))+...
                (1 - alpha)*nchoosek(jj-1, kk)*PPHYsucc*Pa^kk*Pq^((jj-1)-
kk);
            end
        end
    end

end
%THE FIRST ROW [P(j,1)=1 - SUM {P(j,j+1)-P(j,j-k)}]
for(jj=1:M)
    PM(jj,1) = 1 - sum(PM(jj,2:end));
end

Q=PM(1:N,1:N);
R=PM(:,N);

```